Post-print – Please quote as: Hess, D. The value of a dispatchable concentrating solar power transfer from Middle East and North Africa to Europe via point-to-point high voltage direct current lines. Applied Energy, 2018 (accepted)

The value of a dispatchable concentrating solar power transfer from Middle East and North Africa to Europe via point-to-point high voltage direct current lines

Author: Denis Hess[1]*

Dispatchable solar power from concentrating solar thermal power plants (CSP) combined with thermal energy storage and co-firing option can provide energy according to demand. A transfer of such electricity from CSP in desert regions to distant consumer centres may therefore complement domestic energies. A detailed energy system modelling showing the benefit and drawback of CSP from Middle East and North Africa for Europe was not yet done. This paper closes the scientific knowledge gap applying an energy system model with a least-cost approach and detailed scenario analysis for the year 2050. Energy system analyses describe the effects of including and excluding a transfer of CSP from MENA to EU via a grid or via point-to-point high voltage direct current (HVDC) transmission lines. A multi-criteria assessment reveals the impact of such CSP-HVDC power plants on energy infrastructure, operational behaviour, cost and emission of the energy system. To evaluate national grid expansion, a new grid methodology is used as composed of transmission and distribution grid. The evaluation shows that power plant capacity, electrical storage and grid expansion as well as electrical curtailment can cause a beneficial impact when CSP-HVDC is used to supplement the energy portfolio in Europe.

Keywords: CSP-HVDC, EUMENA, energy system model, multi-criteria, DESERTEC

1 Introduction

Concentrating solar power (CSP) combined with thermal storage and co-firing option is one promising dispatchable and low carbon energy technology [1]. Especially in the MENA region, this solar technology is favourable to be implemented in countries with a rising electricity demand in addition to photovoltaics and wind energy. High renewable energy potentials, sparsely populated desert areas are one major advantage for implementing CSP efficiently. In Europe CSP is built in southern Spain, however with limited potential and seasonal unsteady supply. Thus, Europe could supplement its energy portfolio with CSP

[1]Energy System Analysis, German Aerospace Center (DLR), D-70569 Stuttgart, Germany.* Corresponding author e-mail: denis.hess@dlr.de

from MENA due to its limited domestic renewable dispatchable potentials [2] and MENA could profit from income, labour and new living area such as oasis near the power plants. Consequently, Europe as well as MENA could profit from a transfer of dispatchable renewable energy.

1.1 Transfer options, literature review and novelty

For the electricity transfer of CSP from MENA to EU three transmission topologies can be outlined. These are the existing transmission grid, a meshed overlay grid and point-to-point transmission lines. Such infrastructures differ in their capacity, topology, financing and operational behaviour. A point-to-point interconnection is an infrastructure which connects two precise points of a system. In the present case a point-to-point interconnection is defined as a high voltage direct current (HVDC) transmission line between a CSP hotspot in MENA and a demand centre in EU. Point-to-point HVDC and CSP build one power plant and are defined as CSP-HVDC in the following. A meshed overlay grid can be compared to the existing transmission grid with a higher transmission capacity. It is often used in the context of transmitting a high energy amount over a large spatial distance without specific destination such as in Europe [3].

HVDC and CSP are state-of-the-art technologies which are applied worldwide. CSP is often used as dispatchable baseload technology due to its relative cheap thermal storage and almost seasonal constant day-to-day sun cycle in the sun belt area. HVDC is applied as a low-loss electricity transmission technology to transfer electricity over high distances and to interconnect asynchronous power grids [4]. A review of the technical performance of HVDC led to the result that an electricity transfer from North Africa to Europe can improve the dynamic performance of power system in Europe [5]. Public initiatives such as DESERTEC focus to exploit the energy potential of renewable energies in the world's sun belt area for domestic use and for a transfer to high energy consuming regions such as Europe. However, a transfer of a specific type of renewable energy which can be from high value for the destination region was not analysed in detail so far. In the paper at hand an analysis is performed which identifies the advantageous kind of renewable energy and the type of transfer topology with an optimization model at the first time.

Scientific test cases considering the economic comparison of CSP and PV have led to the result that in southern Italy and Egypt CSP is more cost efficient than PV due to its base load character [6]. However, the export of CSP via point-to-point HVDC to Europe with its local competitive renewable energy technologies has not been examined.

Transmission grid studies in Europe by [7] and [8] found out that a transmission grid expansion with the integration of fluctuating renewable energies is beneficial in the long term. However, the use of CSP in MENA for Europe wasn't analysed because the study was limited to Europe. In the case of the meshed overlay grid, former studies used a least-cost approach with an energy system model with high shares of renewable energies in EUMENA (Europe, Middle East and North Africa) with such an infrastructure. They found out that a meshed overlay grid is cost-efficient and therefore often integrated by the used energy optimization model [9], [10]. In these studies, CSP was also integrated in the model. CSP is also analysed in a fully renewable energy system in Texas in the USA regarding the operational behaviour from the system operator viewpoint [11]. However, such optimisation considers predominantly cost and does not lead to the view of other energy system relevant criteria. Showing the impact of a meshed overlay grid on the energy system, a multi-criteria analysis is performed with and without meshed overlay. In the context of CSP, point-to-point transmission infrastructures have been only outlined and described quantitatively in reference [12] and [13]. Point-to-point transmission infrastructures from a CSP power plant to a distant centre of demand have not been analysed in detail in EUMENA with an energy system optimisation model. Showing the effects of point-to-point CSP-HVDC for the energy system, this combined technology is implemented in such a model in the present paper.

Based on the investigation of CSP-HVDC in this paper, the following research questions arise: Is a transmission of dispatchable energy of CSP from MENA to EU beneficial for the composition of an energy system in the year 2050? What benefits and drawbacks in terms of: cost, uncertainty, infrastructural need, operational behaviour such as curtailment and grid stress and also carbon emission result from an energy system that includes such a CSP transfer compared to an energy system that excludes this technological option? Are there tangible alternatives that lead to similar benefits? These novel issues in the field of CSP and system analysis are investigated in a rich system analytic approach showing the value of a CSP transfer from MENA to EU and closing the knowledge gap of an evaluation of CSP-HVDC. Additionally, the effects of using an overlay grid and point-to-point connections are specified. Such transmission infrastructures are essential for the transfer of electricity. It needs to be clarified which option leads to what effect and if a combination of both is appropriate in terms of infrastructural needs and operational behaviour of the energy system. Another novelty consists of applying a new grid methodology for the EUMENA region by [14] which considers node-internal transmission and distribution grids in the system analytic approach. Thus, conclusions of grid expansion inside a region (node) are possible.

The paper is part of the dissertation "The Value of Concentrating Solar Power for a Sustainable Electricity Supply in Europe, Middle East and North Africa" [15].

1.2 Systematic approach

A broad range of scenario analyses is exhibited with the energy system model REMix by linear programming [2], [16], [17]. The approach considers the barriers of the model and tangible technological alternatives of CSP-HVDC critically. Several cost assumptions are used in sensitivity analyses to include future uncertainty of the year 2050. Multi-criteria analyses are represented by the use of different evaluation criteria according to cost, infrastructure, operational behaviour and emission of the energy system (see Table 5) which show scenarios from various perspectives. Such criteria lead to a quantification of the system influence of a transfer of CSP from MENA to EU and the used transmission infrastructure.

In the first part of the analysis the focus is on the overlay grid as a spatial flexibility option in the EUMENA region. Therefore two scenarios are applied. The scenario “Grid OHL” is based on the unlimited expansion of an overlay grid that connects regions in EUMENA (Figure 1a). Such a scenario implies a strong collaboration inside EUMENA. The other scenario “Single OHL” excludes this overlay grid but still uses grid expansion inside the regions (nodal grid expansion) (Figure 1b). This scenario shows an uncooperative EUMENA in that the regions are independent. Both scenarios apply a “greenfield approach”. This term is defined as an approach which does not include the constraints of previous installed power plant capacities. The scenarios are performed with an integration option of all tangible technological options including point-to-point CSP-HVDC, nuclear power plants and CCS (Carbon Capture and Storage), with the same carbon emission limit of 16 g/kWh_{demand} in EUMENA, mean expert cost assumptions and an overhead line (OHL) transmission infrastructure. The scenarios help to detect the influence of an overlay grid under a least-cost optimization and an evaluation of multi-criteria for an energy system with the aim to reach climate protection target with less than 2°C [18].

In the second part of the analysis the focus is on the evaluation of point-to-point CSP-HVDC power plants. The cost input parameters “mean” and an overhead line (OHL) transmission infrastructure are applied in a “partial greenfield” approach. A scenario with high CSP-HVDC capacity penetration is analysed (Figure 1c). This used capacity of CSP-HVDC is reduced systematically in 25% steps till a 100% reduction (Figure 1d). The scenario without CSP-HVDC is the reference. The used overlay grid has limited capacity of transmission lines and can be seen as a higher expanded transmission grid. The transmission line capacities are assumed to be 2 GW for each connection between model regions in the year 2010. The capacity of overlay grid transmission lines expand in the same manner as the demand of the model regions rises from 2010 to 2050. Due to small cost difference among technologies, some technologies can be excluded automatically by the optimization model due to a small cost difference. This so-called “penny flip” effect is a major barrier in optimizing energy systems because it leads to unrealistic results. In order to avoid the possibility of penny flips and disproportional expansion of the overlay grid, the capacities of power plants and storages are exogenously set. They are available in the appendix Table 14 to Table 17. The fundamental barrier of the used REMix is that only cost parameters are used for the optimization. Therefore, the present modelling framework of the scenario has the aim to minimize capacities, and curtailment. This can be achieved, if the demand is covered directly (power to demand) using dispatchable renewable energies. Therefore, the potential of renewable dispatchable energies for each region inside EU is modelled at its limit. The maximum capacity share of CSP-HVDC in EU is designed to achieve a 50% dispatchable energy share, integrating at first the dispatchable renewable energies of each region inside EU. CCS and nuclear plants are excluded due to high cost of nuclear and by reason of insignificant system influence of CCS. The value of CSP-HVDC for the energy system is shown within a multi-criteria analysis.

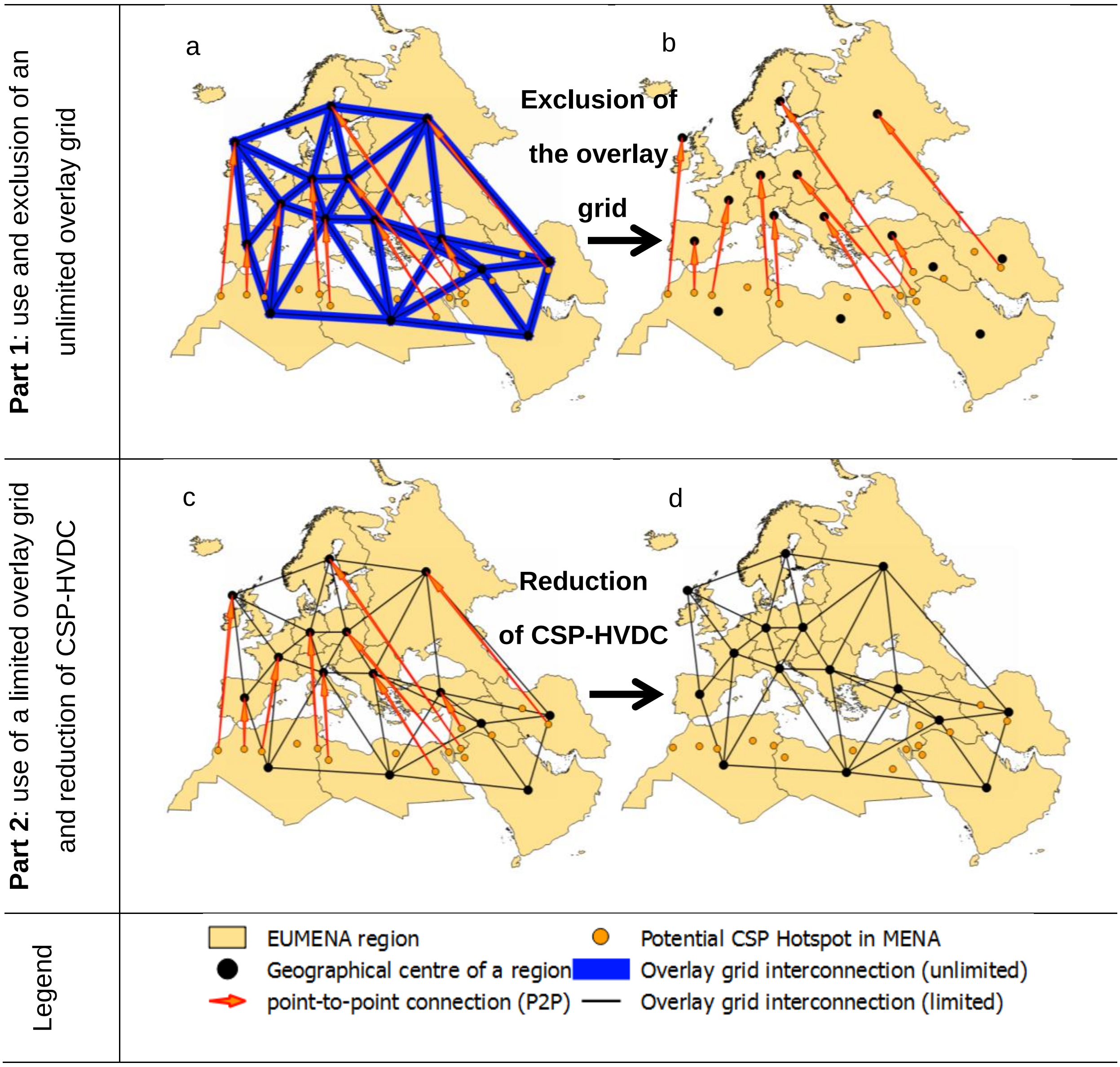

Figure 1: Used overlay grid and CSP-HVDC scheme in the stepwise analysis. The CSP power plants and point-to-point connections from MENA to EU are defined as CSP-HVDC. a) Greenfield optimization possibility of unlimited overlay grid capacities and point-to-point CSP-HVDC capacities, b) exclusion of the overlay grid and optimization possibility of point-to-point CSP-HVDC capacities, c) partial greenfield approach with fixed overlay grid capacities and point-to-point CSP-HVDC capacities, d) reduction of point-to-point CSP-HVDC capacities in 25% steps until complete exclusion.

In the third part of the analysis Germany is investigated as a national example. Here sensitivity scenarios use maximum, medium, minimal cost assumptions as well as overhead lines and underground cables in a “greenfield” approach. This scenario shows future cost uncertainty for an energy mix with shares of dispatchable and fluctuating renewable energies in a 100% renewable energy share [14].

In all scenarios the region internal transmission and distribution grid is included. The model considers the transmission and distribution grid inside a region with representative cost values according to the feed-in capacity of fluctuating renewable energies such as PV and

Wind turbines. Due to its representative character, the model does not consider the power flow inside a region. However, such a novel approach is valuable for the cost optimization considering the grid expansion inside a region. The representative grid model is based on [14], has been validated and gives a robust impression of how and to which extend wind turbines and PV can cause grid expansion. The model can decide whether it is cost advantageous to build new capacities of wind turbines and PV, to feed their capacity into the system or to curtail their energy. The used modelling approach considers in the present paper the grid cost parameters of [14] as a first node-internal grid application of the entire EUMENA region. However, the approach is rather optimistic and still overestimates the grid ability e.g. due to its hourly resolution. The model uses two parameters to quantify the grid: start point of grid expansion in relation to peak load and specific cost per feed-in power of photovoltaics and wind turbines. The used parameters for each model region, distribution and transmission grid are listed in Table 25.

2 Methods

2.1 Energy system model REMix

As a numerical energy system model REMix (sustainable Renewable Energy Mix) [2], [16] and [17] is applied. This bottom-up model has the target function of minimizing system cost (total cost) using linear programming under perfect foresight. System cost include the annuities of investment and the cost of operation and maintenance (O&M), fuel and emission cost for energy relevant technologies (power plants, storage and grid) shown in Eq. (1). REMix consists of two models: REMix-EnDAT (Energy Data Analysis) and REMix-OptiMo (Energy System Optimization). REMix-EnDAT uses climate and weather data to calculate potentials and technological time series of PV, Wind, CSP and hydro power plants. For each region a representative technological time series is the result. In the example of wind onshore turbines REMix-EnDAT uses the wind speed at the level of 132m hub hight and a rotor diameter of 130m. Exclusion areas such as distances to populated areas avoid a distortion of the representative time series. By regarding the cost of technologies, REMix-OptiMo can decide upon configuration and operation of the energy system. This means a quantitative decision about which capacity is built and which dispatch is used. Such an optimization can be performed based on a “greenfield” (model endogenous optimization), a “partial greenfield” (model endogenous optimization under exogenously given capacities) or just a dispatch optimization with only exogenously given capacities. REMix-OptiMo performs the following output data: capacity, generation, system operation, cost as well as emission data. Examples of output data are system cost, regional and technological specific generation and curtailment time series as well as losses and transmission time series between the regions, regional technological and marginal cost, fuel consumption and emission. The model structure is illustrated in Figure 2. REMix is built in the algebraic language GAMS using the CPLEX solver. A detailed overview of the model methods is available in the references [2], [16] and [17]. Due to worldwide available meteorological data, calculated and complied by the German Aerospace Centre, REMix is worldwide applicable. The basic modelling assumptions including the CSP model and all applied and tangible technologies such as renewable energies, nuclear power plants, CCS, coal power plants and gas turbines are explained and characterised in the appendix.

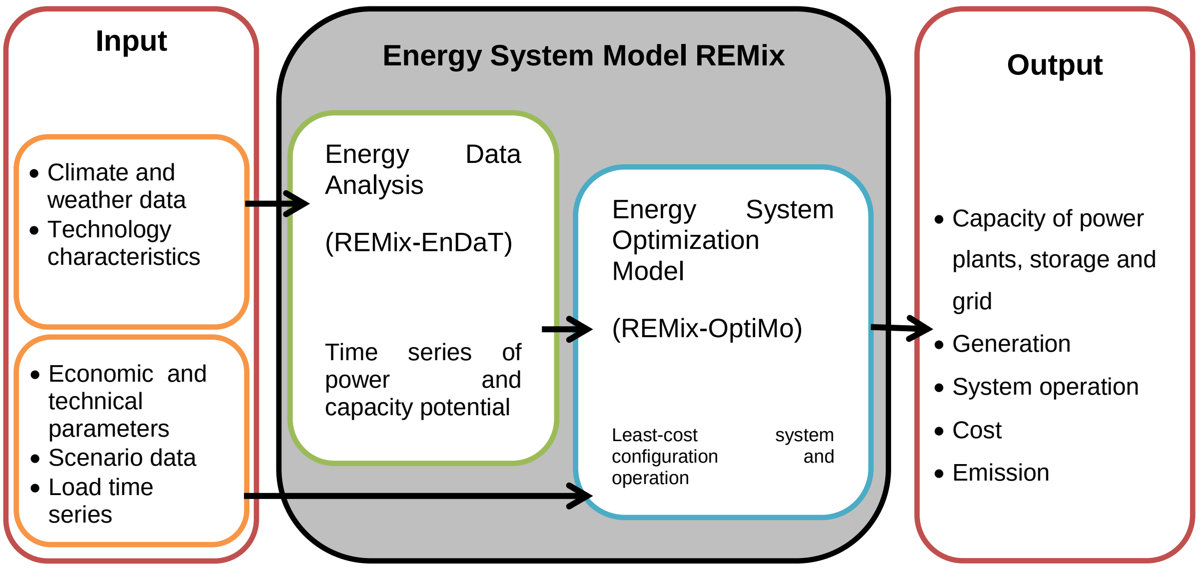

Figure 2: Model structure of REMix-EnDAT and REMix-OptiMo, input and output data based on [17]

Objective function in the linear program framework to be minimized:

$$\sum System\ cost\ [k€]\ \rightarrow min \tag{1}$$

The following equations concretise the system cost and calculation method. REMix, can optimize the variables which are written in bold. System cost is the sum of capital cost $\boldsymbol{C}_{capital}$ and operation cost $\boldsymbol{C}_{operation}$ described in Eq.(5). For the calculation of capital cost the annuity method with the annuity factor $f_{annuity}$ is used including endogenous capacity $\boldsymbol{P}_{addedCap}$ and exogenous capacity $P_{existCap}$ according to Eq. (2) and (3). The annuity factor $f_{annuity}$ considers the interest rate i [%] and the amortization time t_y[years]. The operation cost of the power plant park is calculated using fix and variable O&M as well as fuels and emission cost multiplied with the generated energy of a technology $\boldsymbol{P}_{gen}$ according to Eq. (4).

All cost assumptions in the paper are given in constant monetary value of the year 2015.

$$f_{annuity} = \frac{i \cdot (1+i)^{t_y}}{(1+i)^{t_y} - 1} \tag{2}$$

$$\boldsymbol{C}_{capital} = \left(\boldsymbol{P}_{addedCap} + P_{existCap}\right) \cdot c_{specInv} \cdot f_{annuity} \tag{3}$$

$$\boldsymbol{C}_{operation} = \left(\boldsymbol{P}_{addedCap} + P_{existCap}\right) \cdot c_{specInv} \cdot c_{O\&M\ Fix} + \sum_{t} \boldsymbol{P}_{gen}(t) \cdot \left(c_{O\&M\ Variable} + c_{Fuel} + c_{Emission}\right) \tag{4}$$

$$System\ Cost\ [k€] = \boldsymbol{C}_{capital} + \boldsymbol{C}_{operation} \tag{5}$$

$$= Capital\ Cost + Fix\ O\&M\ Cost + Variable\ O\&M\ Cost + Fuel\ Cost + Emission\ Cost$$

2.2 EUMENA region

The used examination area assessing the value of CSP-HVDC is EUMENA (Figure 3). This geographical region consists of geographical sub-regions: Europe, Middle East and North Africa [19]. Having an impression of the global significance of EUMENA, the population in the year 2015 and 2050 is compared in EU, ME and NA using population data from the UN medium population scenario in Table 1.In the year 2015 the region was inhabited by 1.26bn people and had a global population share of 17.2%. While population of Europe will decrease till 2050 the MENA region will grow strongly according to [20]. Thus, energy demand of MENA countries will rise intensively [21]. However, MENA cannot grow enough to compensate the loss in Europe and the declining global population share of EUMENA with 15.2% in the year 2050. Nevertheless, Europe would even lose more global influence without the MENA region considering its population decline in global population share from 10.3% to 7.5%. Thus, cooperation could be a WIN-WIN for all EUMENA sub-regions stabilising the region in social issues but also profiting from environmental, economic and institutional affairs. An exchange potential rises therefore also in other fields beyond energy.

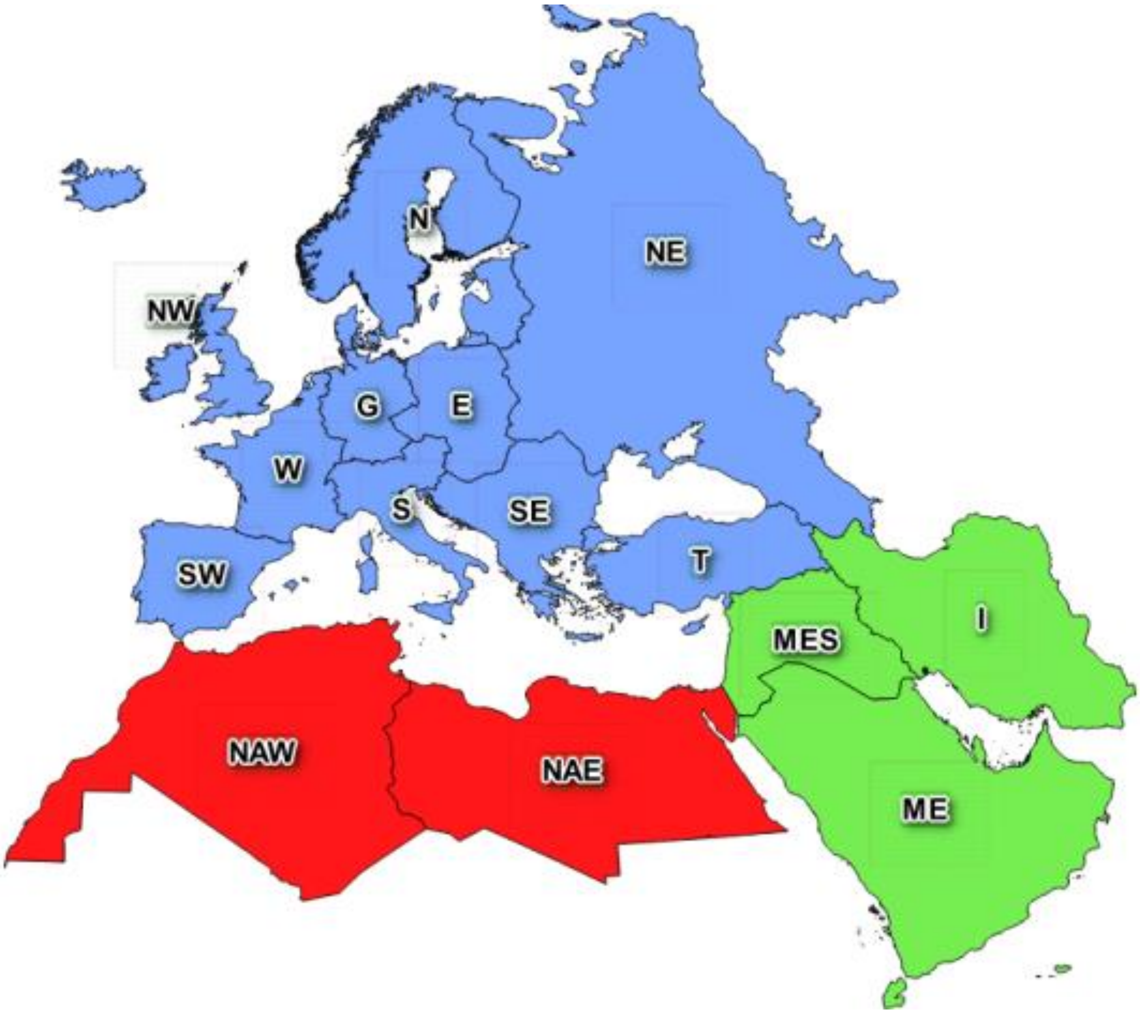

Figure 3: EUMENA geographical map [22]

Table 1: Population data in EUMENA and the world

Population data [20]				
Region	**Population [bn]**		**Global population share**	
year	2015	2050	2015	2050
World	7.35	9.73	100%	100%
EUMENA	1.26	1.47	17.2%	15.2%
EU*	0.76	0.73	10.3%	7.5%
ME	0.32	0.47	4.3%	4.8%
NA	0.18	0.27	2.5%	2.8%

*Russia until Ural Mountains is assumed with 75% of population in Russian Federation [23]

In Figure 3 the 15 analysed regions inside EUMENA are illustrated. An aggregation inside such regions is made due to computational constraints of the used energy system model. In the following Table 2 the spatial aggregation for the model regions of Figure 3 is shown. The spatial focus of the analysis is not only on the entire EUMENA region but also on sub-regions and nations, wherefore Germany is used as a national example.

An aggregation of separate nations can lead to a smoothing of their demand and resource characteristic. To reduce such falsification an aggregation is at first made according to a similar distribution of demand. Secondly the aggregation is made to limit the east-west expansion of a region avoiding an excessive smoothing of solar resources. Depending on the spatial proximity of a model region to Germany, the model regions close to Germany have a smaller spatial area than the distant model regions. This allows a better model framework to cope with a higher influence of the surrounding regions for Germany.

Table 2: Aggregation of countries to 15 model regions in the examination area EUMENA

Model region	**Alias**	**Country or region**
G	Germany	Germany
N	North	Denmark, Norway, Sweden, Finland, Lithuania, Latvia, Estonia
E	East	Poland, Czech Republic, Slovakia, Hungary
S	South	Switzerland, Austria, Liechtenstein, Italy, Slovenia
W	West	France, Belgium, Netherlands, Luxemburg
NW	North West	United Kingdom, Ireland, Iceland
NE	North East	Ukraine, Moldova, Belarus, Russia until Ural mountains, Azerbaijan, Armenia, Georgia
SE	South East	Greece, Croatia, Rumania, Serbia, Kosovo, Albania, Macedonia, Bulgaria, Bosnia-Herzegovina, Montenegro
SW	South West	Portugal, Spain
T	Turkey, Cyprus	Turkey, Cyprus
MES	Mesopotamia	Israel, Jordan, Palestine, Lebanon, Syria, Iraq
I	Iran	Iran
ME	Middle East	Djibouti, Yemen, Oman, Saudi Arabia, UAE, Qatar, Bahrain, Kuwait
NAE	North Africa East	Libya, Egypt
NAW	North Africa West	Morocco, Algeria, Tunisia

2.3 Modelling of CSP-HVDC in REMix

2.3.1 *CSP-HVDC*

A CSP-HVDC power plant is modelled with a solar field (SF), thermal energy storage (TES), power block (PB) with co-firing system (BUS), two HVDC converters and a HVDC transmission. Each of these components has its own techno-economic characteristics which are listed in Table 18 and Table 23 and are considered by the REMix model. The following description is based on [17] and reveals the functioning of the CSP model with thermal storage and co-firing option in REMix.

The total solar field thermal capacity is composed of the exogenous capacity $Q_{existCap}$ and the model endogenous capacity $\boldsymbol{Q}_{addedCap}$ and is limited to the total potential calculated by REMix-EnDAT. The solar field thermal output $\boldsymbol{Q}_{SF}(t)$ arises from the overall capacity $(\boldsymbol{Q}_{addedCap} + Q_{existCap})$ and the normalised hourly availability of the solar resource $s_{gen}(t)$ as thermal time series. This is described in Eq. (6).

$$\boldsymbol{Q}_{SF}(t) \overset{!}{=} (\boldsymbol{Q}_{addedCap} + Q_{existCap}) \cdot s_{gen}(t) \qquad \forall t \qquad (6)$$

[17]

The thermal balance of CSP plants includes the thermal output of a solar field $\boldsymbol{Q}_{SF}(t)$, backup unit $\boldsymbol{Q}_{BUS}(t)$, TES charging $\boldsymbol{Q}_{charge}(t)$ and discharging $\boldsymbol{Q}_{discharge}(t)$, the thermal curtailment of the solar field $\boldsymbol{Q}_{curtail}(t)$, the power generation of the power block $\boldsymbol{P}_{gen}(t)$ according to Eq.(7) and the efficiency of the power block $\eta_{generator}$. The efficiency of the power block is the product of the thermal and electrical efficiency.

$$\boldsymbol{Q}_{SF}(t) + \boldsymbol{Q}_{BUS}(t) + \left(\boldsymbol{Q}_{discharge}(t) - \boldsymbol{Q}_{charge}(t)\right) - \boldsymbol{Q}_{curtail}(t) \overset{!}{=} \frac{\boldsymbol{P}_{gen}(t)}{\eta_{generator}} \qquad \forall t \qquad (7)$$

Hourly changes in TES energy level $\boldsymbol{U}_{level}(t)$ are described by the storage balance, which accounts for charging, discharging, and self-discharging in Eq.(8). An additional equation sets the storage level in the first and last time step to the same value, assuring that no energy is produced in the storage [17].

$$\boldsymbol{U}_{level}(t) \overset{!}{=} \boldsymbol{U}_{level}(t-1) + \left(\boldsymbol{Q}_{charge}(t) \cdot \eta_{charge} - \frac{\boldsymbol{Q}_{discharge}(t)}{\eta_{discharge}}\right) \cdot \Delta t - \frac{1}{2} \cdot \left(\boldsymbol{U}_{level}(t) + \boldsymbol{U}_{level}(t-1)\right) \cdot \eta_{self} \quad \forall t \tag{8}$$

The hourly output of the power block $\boldsymbol{P}_{gen}(t)$ is limited by the available capacity. The storage level $\boldsymbol{U}_{level}(t)$ must be in all time steps lower than the overall TES capacity [17].

The novelty of modelling does not consist in the CSP model - developed by [2], [24] and [17] - but in the method of implementing CSP-HVDC in the REMix model. A CSP-HVDC power plant transmits electricity via HVDC point-to-point transmission line directly to one offtaker in Europe. Thus, for this offtaker CSP is available apparently locally like home-grown renewable energies. Therefore CSP-HVDC is modelled as a power plant which has the solar resource of a MENA country and HVDC transmission losses - occurring with the transmission of CSP generated electricity to the consumer - but CSP from MENA is placed virtually in a European region. The gross capacity of the HVDC line $P_{HVDC,gross}$ is the same as the net capacity of the CSP power block $P_{PB,CSP,net}$ as described in Eq. (9).

$$P_{PB,CSP,net} = P_{HVDC,gross} \tag{9}$$

Transmission losses are assumed to increase linearly with an increasing distance.

2.3.2 *CSP sites, HVDC point-to-point transmission corridors and offtaker points*

The basis for the CSP-HVDC power plant modelling is built by an exemplary identification of 15 CSP sites (hotspots) in MENA and 82 potential offtakers in geographical Europe (Figure 7 and Figure 8). These production and offtaker centres define the starting and end point of a CSP-HVDC power plant in the model. CSP hotspots are chosen selecting good solar resource [25], short distance to Europe and diversified placement in different MENA countries. The CSP resource is taken within a 30km radius of the hotspot. Offtakers are bigger EU cities that represent centres of demand.

The pathways of HVDC between these CSP hotspots and offtaker are calculated using a line laying algorithm [26]. This algorithm considers the geographical terrain with cost and minimizes cost to find a cost optimal pathway. Its spatial resolution is 1km x 1km.

The transmission pathway is calculated according to excluded areas (highest cost), preferred and unprivileged areas (lower or higher cost). Here two geographical categories are essential: The first category is independent from the direction of a pathway which is called isotropic friction image. The second category is dependant from the direction of the pathway and called anisotropic friction image (such as slope). With both categories cost-distance images of the CSP hotspots are calculated. Including the offtaker (demand centre) in the analysis, a cost optimal pathway can be calculated with the cost-distance image.

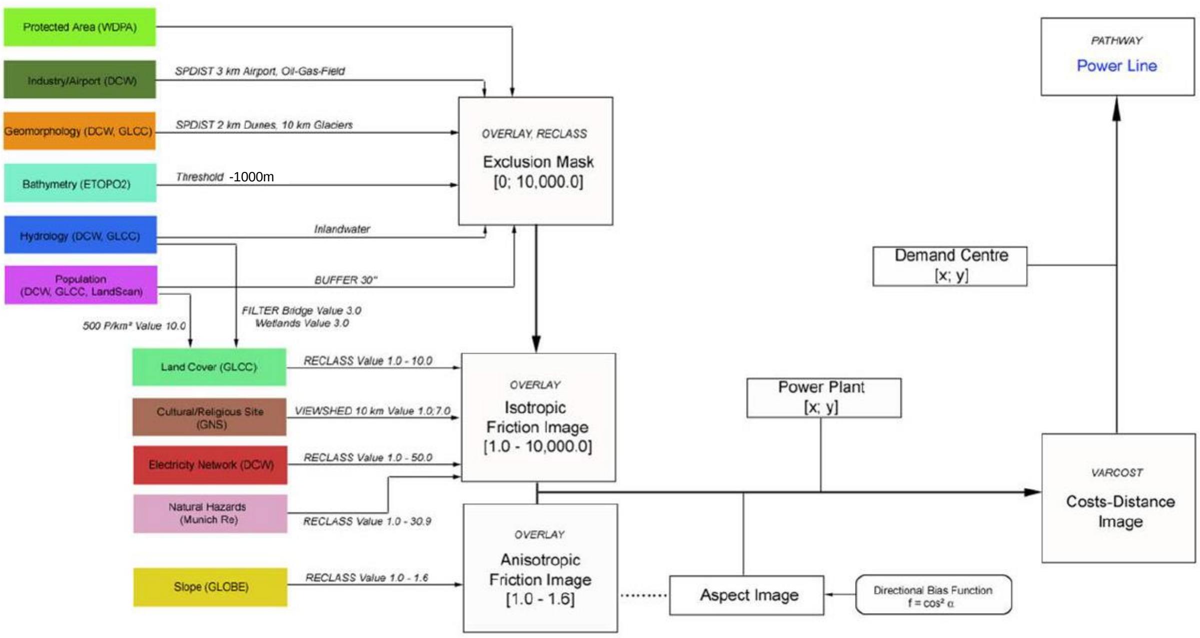

Figure 4: Line laying model based on [26]

The used isotropic friction images are exhibited in Figure 5 and Figure 6 showing two cost sensitivities:

- In Figure 5 a business as usual cost assumption is assumed which leads to predominant onshore pathways as shown in [26] and [25].
- In Figure 6 a dominant use of offshore pathways results. Here the isotropic friction image was calculated like in Figure 4 but with an addition of its highest sea cost value (~40) to the existing cost assumption of the land area.

Out of all possible combinations with 15 CSP sites and 82 potential offtakers (1230 possibilities) those CSP-HVDC plants are chosen which have a short distance to the consumer and at the same time a diversified solar resource from different CSP sites. Both figures illustrate the same connections between CSP hotspot and offtaker with different pathways. Evaluating CSP-HVDC in this thesis with an energy system model presumes a reduction of this high-resolution infrastructure due to computational limits. Thus, average transmission lengths and average solar resource from selected CSP-HVDC are used each for one model region. The total average length to one model region is between 1200km and 3800km and is listed in Table 3. The average solar resource is shown by full load hours of the solar field in Table 13. These solar resources of the CSP hotspots are assumed as relative conservative compared to the spatial average solar resources of a model region.

Figure 7 and Figure 8 illustrate a possible topology of CSP-HVDC. It is visible that in Figure 8 more straight pathways occur than in Figure 7 due to total higher cost. Thus, it can be assumed that Figure 8 represents sea cable and also underground cable. The CSP power plant sites and offtakters are exemplary and do neither represent real projects nor feasibility studies.

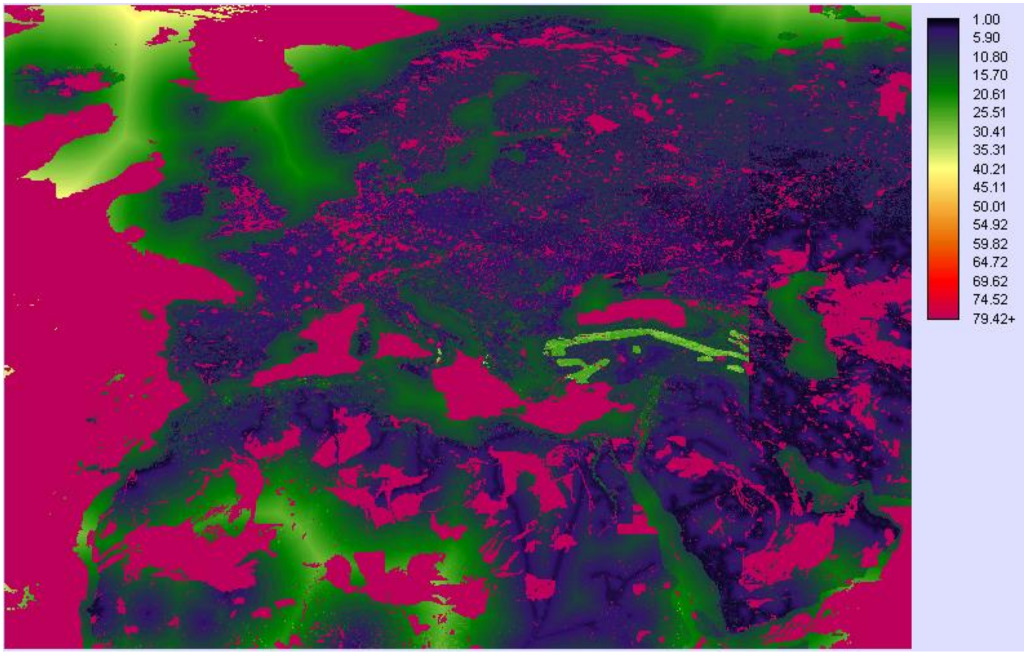

Figure 5: Isotropic friction image based on [26] (OHL case)

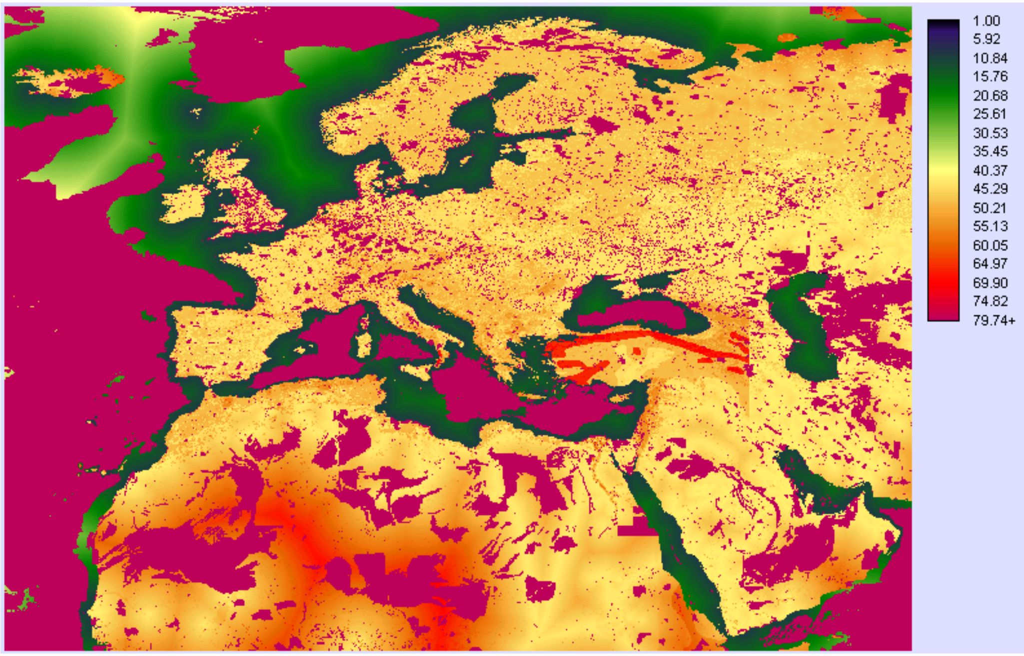

Figure 6: Isotropic friction image based on [26] with addition of highest sea cost value (~40) to all land cost values allowing the algorithm to use predominantly offshore pathways (sea cable and UGC case)

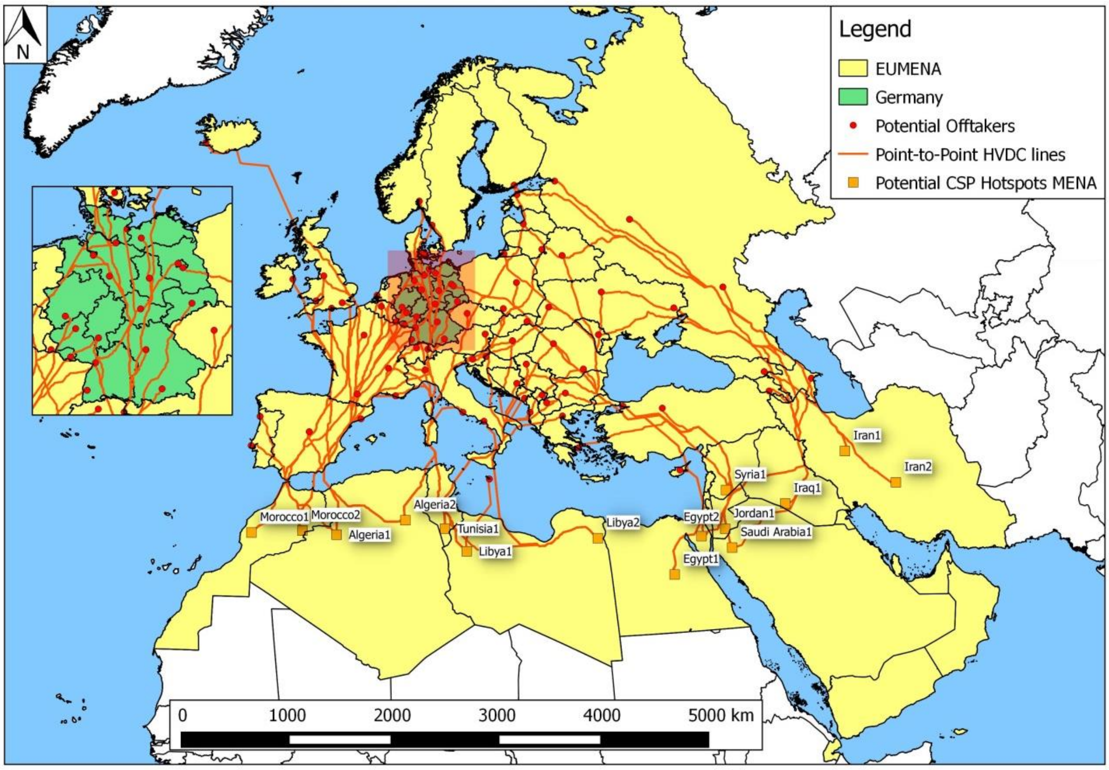

Figure 7: Point-to-point CSP-HVDC with potential CSP hotspots in MENA and potential offtakers in Europe – predominant onshore line configuration (OHL case)

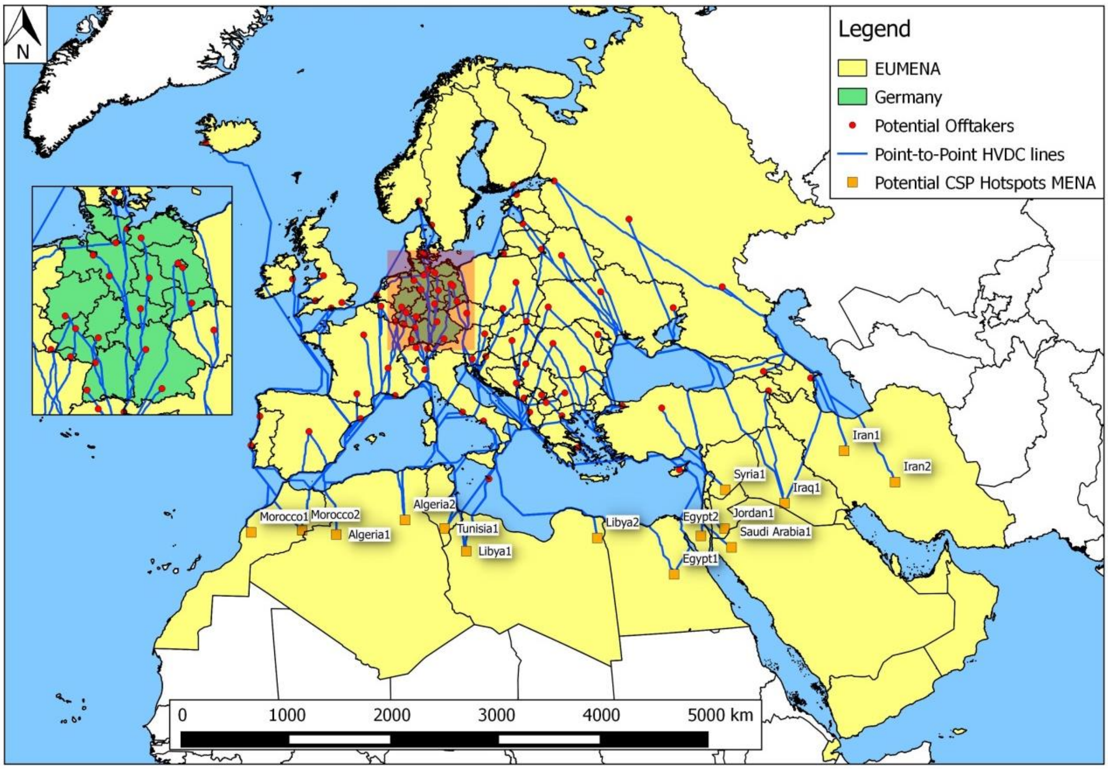

Figure 8: Point-to-point CSP-HVDC with potential CSP hotspots in MENA and potential offtakers in Europe – predominant offshore configuration (sea cable and UGC case)

For Germany a relatively high number of offtakers is included to identify precisely the average length of a specific point-to-point line.

Table 3: CSP-HVDC transmission line lengths to model regions as potential offtakers

Model region	**Predominant OHL configuration**		**Predominant sea and UGC configuration**		**Total average length of point-to-point line**
	Length line land	Length line sea	Length line land	Length line sea	
G	2343	249	1212	1403	2604
N	3461	331	1675	1915	3691
E	2549	356	1104	1626	2818
S	1540	366	568	1321	1898
W	2178	214	1012	1318	2361
NW	2747	930	645	3291	3807
NE	2502	109	1342	1129	2541
SE	1928	441	587	1604	2280
NAE	0	0	0	0	0
NAW	0	0	0	0	0
SW	1206	88	521	846	1331
T	899	255	406	838	1199
MES	0	0	0	0	0
I	0	0	0	0	0
ME	0	0	0	0	0

By analogy point-to-point transmission lines for hydro reservoir power plants are determined which are going from model region **N** in Figure 3 to the nearest surrounding model regions **G**, **E** and **NW** in Figure 3. Due to the high potential in model region **N** and current initiatives using hydro reservoir from Norway for some European countries, this technological option is included as one European home-grown energy resource. Pathway length and the assumed distribution of hydro reservoir capacity to the model region **G**, **E** and **NW** are shown in Table 4. The model regions of Table 3 are defined in Table 2.

Table 4: Link lengths of point-to-point hydro reservoir (not optimized by line laying model)

From potential exporting model region	**To potential offtaker model region**	**Total length [km]**	**Sea cable section [km]**
N	G	1570	160
N	E	1704	350
N	NW	2502	850

2.4 Multi-criteria analysis

Evaluation criteria are chosen in Table 5 to clarify other relevant energy systemic criteria beside cost that have an impact of the energy system regarding infrastructure, operational behaviour, cost and emission. These evaluation criteria build the basis of this paper to assess scenarios. To compare the criteria among regions, the data are specific per **annual** electricity net demand.

Table 5: Analysed evaluation criteria

Evaluation criteria	**Unit**	**Description**
Power Plant Capacity	[GW/TWh]	All power plants plus the electrical discharge capacity of P2G2P and hydro reservoir
Electrical Storage Capacity	[GW/TWh]	Electrical storage charge capacities
Curtailment	[TWh/TWh]	Electrical curtailment of photovoltaic, wind turbines, hydro run off river and hydro reservoir
Power Kilometre	[TWkm/TWh]*	Capacity of a power line multiplied with its length. Power km of grid, node internal transmission and distribution grid and point-to-point infrastructure – the power km of the grid connections between model regions are divided equally between these regions.
System Cost	[€/kWh]	Capital cost, fix and variable O&M cost, fuel cost and emission cost
Carbon Emission	[g/kWh]	Carbon emission of coal, lignite and natural gas during fuel conversion into electricity

*Capacity of power kilometre (TWkm) and annual electricity demand (TWh) can't be reduced in a fraction due to their different characteristic!

3 Results

3.1 Results Part 1

Figure 9 shows the results with the integration of the overlay grid (Figure 9a) as well as its exclusion (Figure 9b) in EUMENA. Figure 9a illustrates with the blue lines an expansion of transmission lines of the overlay grid. Up to 85GW from model node **NW** to model node **W** can occur. Transmission lines are expanded more in north-south direction than in east-west direction. Interconnections between **NAW**, **NAE** and **ME** are assessed as insignificant by the model. Both figures show also the grid expansion inside the model regions. This so-called node-internal grid expansion of the transmission and distribution grid in Figure 9a illustrates a high expansion in some regions and in Figure 9a an almost equally distributed expansion in every model region. The power kilometre subdivision in Figure 9a shows that CSP-HVDC is not integrated using an overlay grid. The exclusion of the overlay grid leads to the integration of CSP-HVDC. Thus, for the scenario “Grid OHL” it can be questioned if CSP is built in MENA and then transmitted using the overlay grid? Therefore a correlation analysis is done comparing power generation of different renewable energy technologies and the transmission line usage between selected model regions. This correlation analysis investigates the probability of the hourly energy production of a power technology and the hourly use of a selected transmission line of the overlay grid. Positive values near to 100% mean a high correlation (export), negative values indicate an anti-correlation (import).

Table 6 shows the results of the correlation analysis. The time series of CSP electricity in model region **NAW** and the transmission from **NAW** to western EU offer a high correlation of an export form this technology to the model regions **SW**, **W** and **NW**. The correlation of Wind Onshore electricity in model region **NW** and the transmission from **NW** to western EU and North Africa feature a high correlation of an export from this technology to the model regions **W**, **SW** and **NAW**. Other correlations do not show a comparable extent. The results show that CSP is highly suitable for an export from North Africa to Western Europe using an overlay grid.

Table 6: Exemplary correlation of hourly model output time series from generation out of CSP, PV, Wind Onshore and Wind Offshore in NW and NAW with hourly model output time series of transmitted electricity

Electricity generation in	Transmission line / export from - to	CSP	PV	Wind Onshore	Wind Offshore	Sum PV and Wind
NW	NW-W	-	-43%	90%	28%	90%
NW	W-SW	-	-37%	54%	27%	54%
NW	SW-NAW	-	-26%	37%	11%	37%
NAW	NAW-SW	76%	12%	-1%	1%	9%
NAW	SW-W	72%	22%	-10%	-9%	9%
NAW	W-NW	49%	22%	-14%	-6%	5%

Green colours reveal a high correlation, red colours show an anti-correlation. Yellow colours indicate no correlation.

Having a look on the evaluation criteria in Figure 10, it is remarkable that the two scenarios do not distinguish much in system cost but in almost every other criterion. The use of the overlay grid is about 7% more cost-efficient. Compared to the scenario “Single OHL” the scenario “Grid OHL” reduces power plant capacity to about 13%, storage capacity to about 272% and curtailment to about 34%. However, it causes a significant increase of power kilometre with about 176%. Thus, small cost changes can lead to a recognizable change in all other parameters of an energy system. A least-cost approach can therefore be helpful comparing scenarios with other evaluation criteria on the same least-cost level. As shown in this analysis, alternatives are essential for a comparison of scenarios. Otherwise a least-cost approach can also lead to misinterpretations if comparable alternatives and sensitivities are missing! The major problem of a cost optimization model is that such minimal cost differences can’t be seen if only one scenario is applied. Therefore, it is important to show the extreme guardrails of scenarios to get an impression of the sensitivity of the results. The option of the overlay grid is chosen in the scenario because it is more cost-efficient to balance energy over a spatial area than building electrical storages or curtail power plants. However, the need of such a large capacity expansion of power lines is arguable due to social, political and organisational barriers. A limited overlay grid may be more appropriate reducing power kilometre still allowing the reduction potential of needed power plant and storage capacities as well as less curtailment. Such a grid is therefore used in the second part of the analysis.

Free grid interconnections (Grid OHL):	**Isolated model regions (Single OHL):**
sum 1457 TWkm	**sum 528 TWkm**

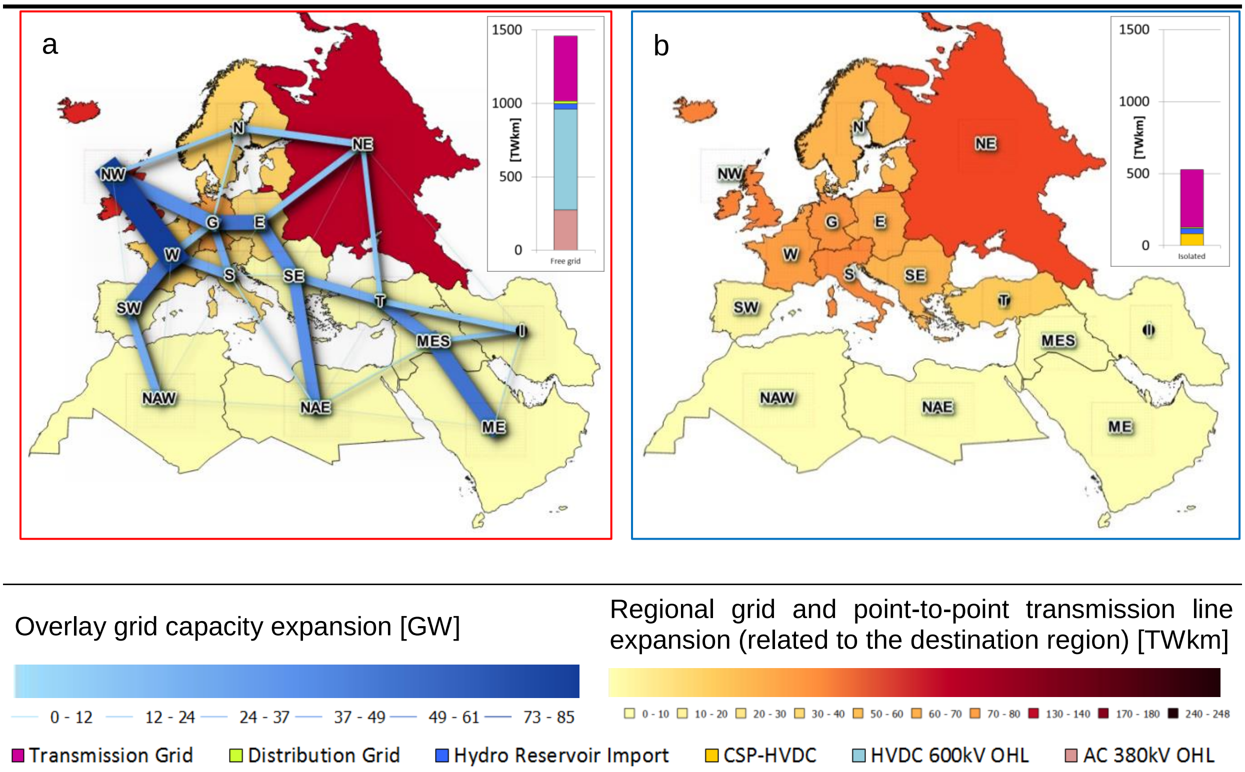

Figure 9: Comparison of grid expansion in GW of overlay grid transmission lines and TWkm. A scenario with unlimited overlay grid interconnections (a) is compared to a scenario with isolated model regions with the exclusion of the overlay grid (b). The regional grid expansion possibility of transmission and distribution grid (nodal grid) and CSP-HVDC integration option is included in both scenarios.

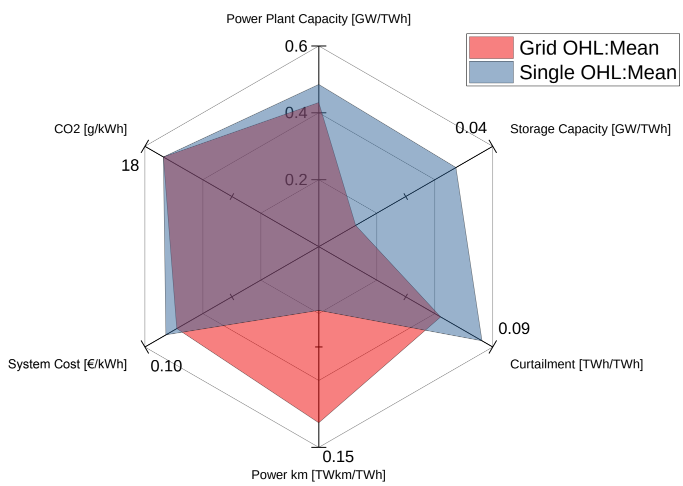

Figure 10: Grid vs. Single. An unlimited grid expansion is a cost-efficient way but causes the need of many power km over EUMENA. Compared to the scenario without overly grid there is only a cost reduction of about 7% but a power km increase of about 176%. Due to spatial flexibility using an overlay grid the energy system needs less power plant capacities, storages and causes less curtailment.

3.2 Results Part 2

The radar charts in Figure 11 constitute the results of the analysed evaluation criteria for the overall region EUMENA, the sub-regions EU, MENA and on national scale the region of Germany. The ochre charts are the analysed CSP-HVDC scenarios (base and 50% CSP-HVDC capacity reduction). The grey charts represent the reference scenario without CSP-HVDC. The results are analysed to show the reader the value and impact of CSP-HVDC with different shares and the consequence of the exclusion of this technology in different regions. The impact of the energy system can be evaluated when summarizing all evaluation criteria. In other words regarding the radar charts show that the smaller the area is, the lower is the impact. For a suitable quantification of the impact of each criterion there is still no answer to the open question how to scale the evaluation criteria in the right relation to each other. In this analysis each evaluation criteria is scaled according to a value near the maximum. This allows assessing the criteria in the same relation to each other. Also a comparison of the analysed regions can be drawn due to the same specific scale (per annual net electricity demand) of the evaluation criteria in each region.

Figure 11a and Figure 11b show the EUMENA region. It is visible that the missing of CSP-HVDC leads to a higher need of power plant and electrical storage capacities and causes more electrical curtailment. However, more power kilometre may be needed due to long distances with CSP-HVDC (keeping in mind an optimistic modelling of the transmission and distribution grid power km). Regarding the area of the radar charts, it is obvious that scenarios with CSP-HVDC lead to smaller areas. In Figure 11c-f the focus is on a more regional scale considering EU and MENA separately. It is evident that the MENA region has lower specific values in all categories than in the EU region except specific CO_2 emission. Due to the local possible use of dispatchable CSP, it may be easier for MENA to implement a low carbon energy system compared to the EU region.

CSP-HVDC is used per definition in the analysis only for EU. However, different results for MENA do occur when neglecting this technology. The reason therefore is that all regions are interconnected with a grid which leads to an interdependency among the regions. As described in section 1.2 the meshed overlay grid has fixed transmission capacities which are quantified in the appendix in Table 17. Another reason of the different results in the MENA region is the global CO_2 emission limit which leads to a regional optimization of CO_2 emission. This regional optimization of CO_2 emission leads to a different power plant commitment. The results in Figure 11e show that a use of CSP-HVDC leads to higher CO_2 emission in MENA and consequently lower CO_2 emission in Europe. This means that the power plant commitment in the EU is more effective to avoid CO_2 using CSP-HVDC. Thus, the region EU contributes to a higher degree of freedom for CO_2 emissions in the MENA region with an integration of CSP-HVDC for the EU. Nevertheless, the specific CO_2 emission is already low and the difference between EU and MENA has not a significant impact.

For a national view towards the results, Figure 11g and Figure 11h display the evaluation criteria for the model region of Germany. This region has the highest specific values compared to EU and MENA and therefore generates a higher impact on its energy system. In the case of the use of CSP-HVDC all evaluation criteria are smaller except the power kilometre. Reducing CSP-HVDC capacity leads to a dominant increase of electrical storage capacities and curtailment.

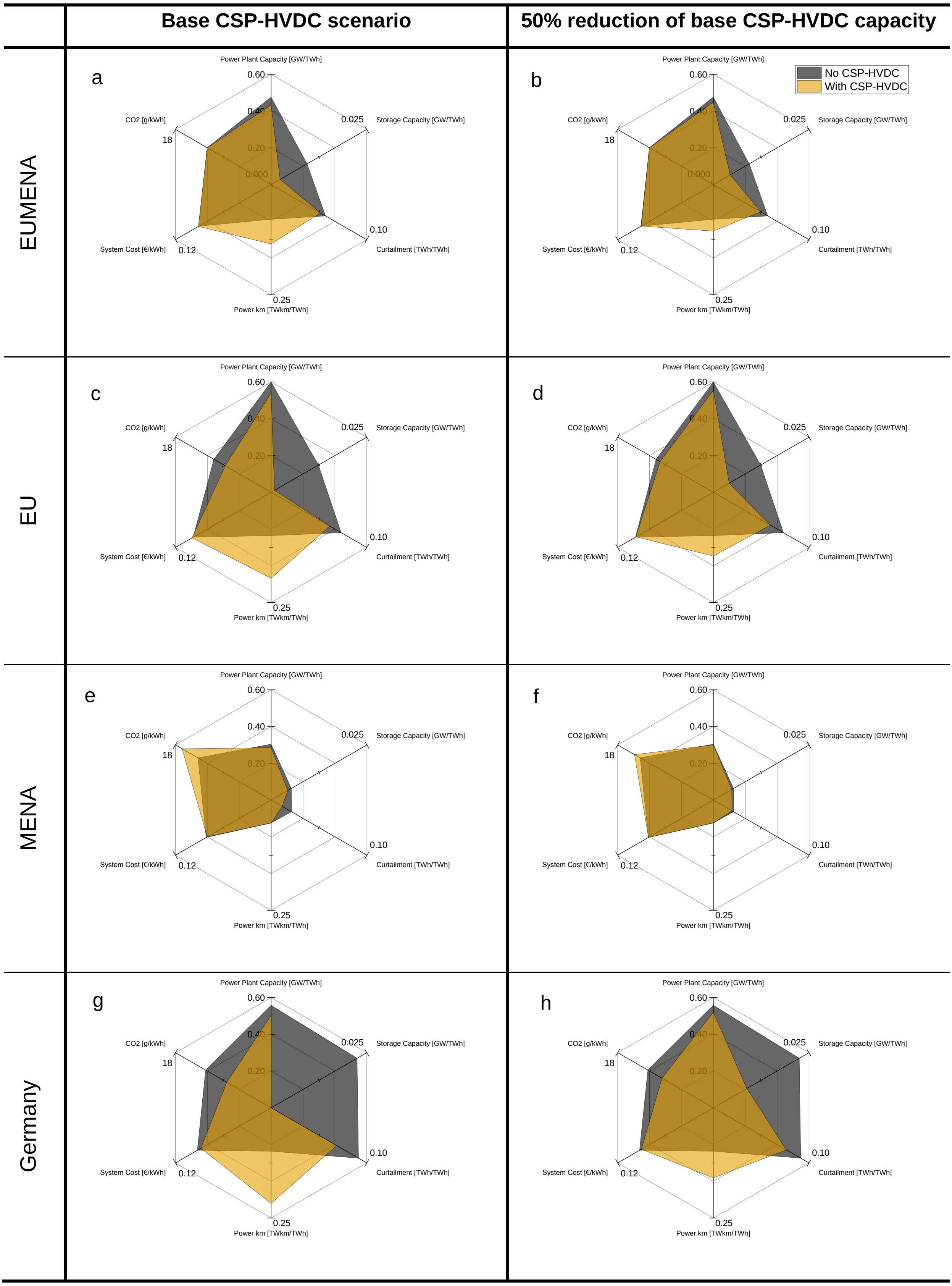

Figure 11: Radar charts showing the value of CSP-HVDC. Base scenario is shown in the left column in ochre, 50% reduction of CSP-HVDC capacity of base scenario in the right column in ochre. Grey radar charts show an energy system without CSP-HVDC as reference. Specific evaluation criteria per annual net electricity demand of each region are applied.

3.2.1 *Grid and transmission Infrastructure*

Figure 12 exhibits the power km over EUMENA according to grid infrastructure categories (overlay grid, P2P and nodal grid). The power kilometres of the overlay grid are fixed. A reduction of CSP-HVDC leads to lower total power km. However, such a reduction of dispatchable energy leads to an increase of nodal grid expansion of transmission grid (red double arrow in Figure 12 and visible in Figure 13) due to higher fluctuating energy shares of Wind and PV. The distribution grid is not expanded and its stock is not listed due to unknown data. Missing CSP-HVDC also leads to a higher use of hydro reservoir import capacity over point-to-point lines (dark blue bulk) from model region **N** to **NW**, **G** and **E.** Such an increase indicates a need of dispatchable energy.

Lower CSP-HVDC shares can also reduce total power kilometre because nodal grid power kilometre increase. This potential trade-off can be achieved in the analysed case with an adequate share of CSP-HVDC. Such a share can therefore lead to a reduction of total power kilometre. This characteristic is visible in Figure 14 with the falling gradient of CSP-HVDC (P2P lines) and the rising gradient of the transmission grid (nodal grid).

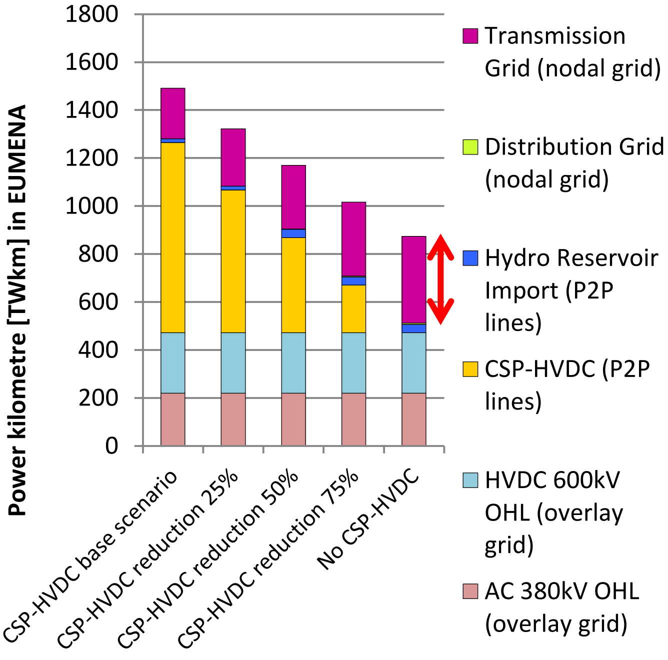

Figure 12: Different shares of CSP-HVDC capacity and resulting expansion of power kilometre according to transmission infrastructure categories

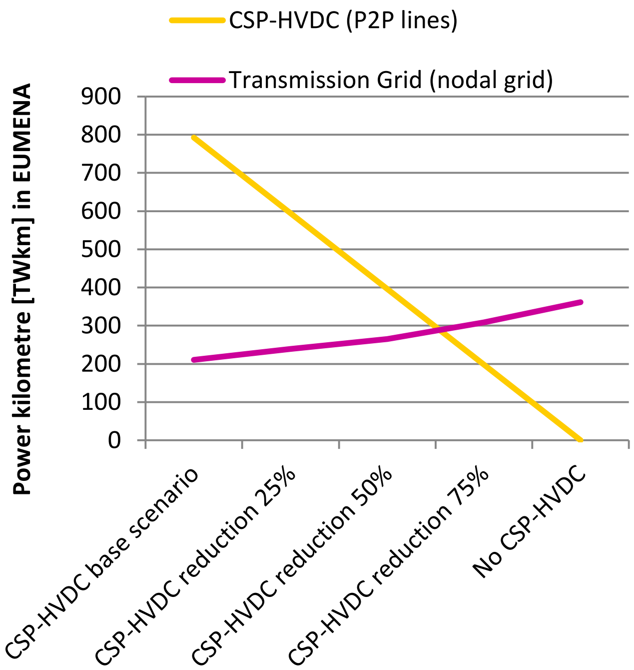

Figure 13: Trade-off of power kilometre between CSP-HVDC (P2P lines) and Transmission grid (nodal grid) in EUMENA

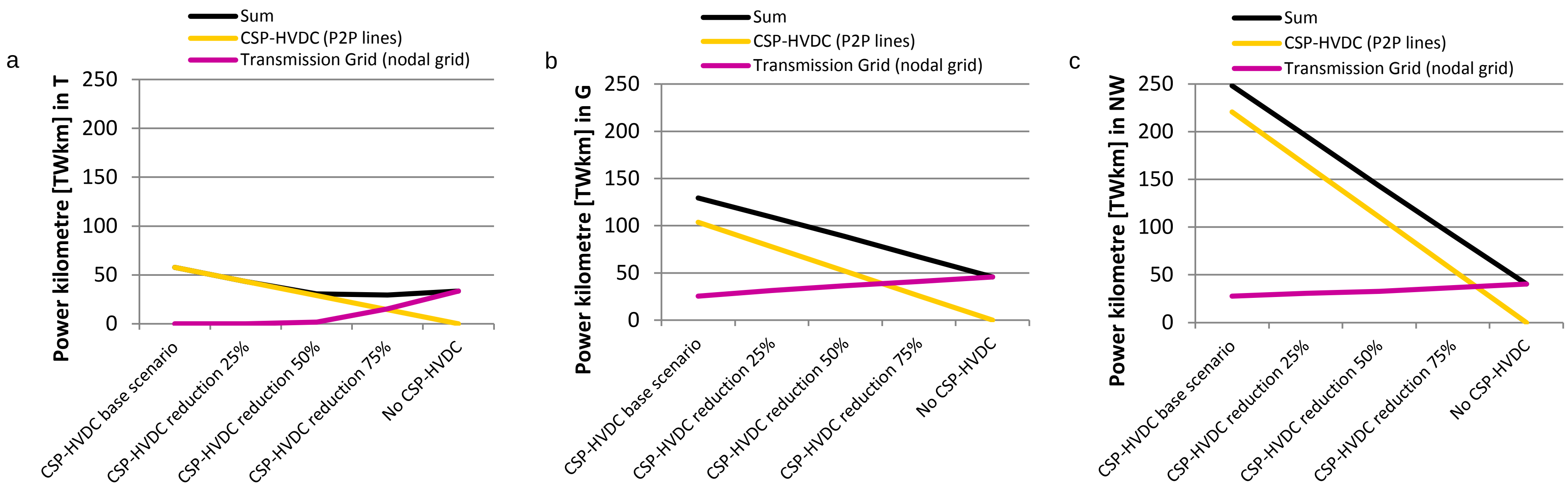

Figure 14: Trade-off of power kilometre between CSP-HVDC (P2P lines) and Transmission grid (nodal grid). In (a) of model region T**, in (b) of model region** G **and in (c) of model region** NW

If the rising gradient of the transmission grid is higher than the falling gradient of CSP-HVDC a reduction potential of total power kilometre occurs. This reduction is also visible with the sum of both shown power kilometre categories. Figure 14a reveals that gradient of transmission grid is higher than the gradient of CSP-HVDC in model region **T**. Thus, including CSP-HVDC can reduce total power kilometre. The northern the region the higher is the gradient of CSP-HVDC due to higher distance between CSP and offtaker. This is visible in Figure 14b with model region **G** and in Figure 14c with model region **NW**. Thus, the reduction potential of total power kilometre decreases in the northern model regions. However, the grid model is conservatively calibrated and bears a potential higher gradient of the nodal grid than assumed! Thus, more northern regions may profit from a reduction of total power kilometre. A reduction of nodal grid power kilometre can be achieved in almost every model regions and reduces therefore the effort in building new transmission lines spread inside a spatial area. The power kilometre of CSP-HVDC outside the territory of an offtaker model region should be designed as a cooperative project to involve affected people by decision making and financial aspects [13].

3.2.2 *Utilisation of the transmission grid*

In this section the influence of point-to-point CSP-HVDC power plants on the operation of the overlay grid with limited capacity is analysed. The overlay grid is the combination of all AC and DC interconnections between the model nodes. The focus of the analysis is the comparison of average utilisation and the number of capacity peaks of transmission lines in the transmission grid.

The results in Table 7 show that higher shares of CSP-HVDC can lead to a reduction of the average utilisation and a reduction of capacity peaks of the overlay grid. Thus, an integration of CSP-HVDC yields a protective effect for the overlay grid against high stress.

Table 7: Comparison of the overlay grid utilisation

Grid utilisation	**CSP-HVDC base scenario**	**-25% CSP-HVDC**	**-50% CSP-HVDC**	**-75% CSP-HVDC**	**No CSP-HVDC**
Reduction of average utilisation	11%	2%	-7%	-3%	Reference
Reduction of capacity peaks* in link flow direction	29%	18%	11%	5%	Reference
against link flow direction	14%	10%	7%	4%	Reference

*Peak is defined as 95% of max. link capacity

The negative values in Table 7 are outliers and indicate a lower grid utilisation reduction compared to the reference “No CSP-HVDC”. However, the trend of a higher grid utilisation reduction with higher CSP-HVDC shares is evident.

3.2.3 *Combination of overlay grid and point-to-point CSP-HVDC*

Overlay gird and point-to-point CSP-HVDC power plants can both reduce power plant and electrical storage capacity and curtailment of the energy system to about same energy system cost. The major difference is the increasing stress of the overlay grid when CSP-HVDC is not integrated (Table 7). One of the results of the REMix model is an overlay grid with a huge transmission capacity expansion (Figure 10). Such a massive overly grid capacity is due to its assumed minimal cost characteristic and does not integrate CSP-HVDC in that framework (Figure 9). However, CSP is used for a transmission via the overlay grid from MENA to EU (Table 6). This result of the model means that CSP in MENA is beneficial for the use in EU. However, the building of such a huge overlay grid is unrealistic especially as a first step. The major barrier of building an overlay grid is its unclear financing and operation over a large spatial area. As a first step it might be easier to implement point-to-point CSP-HVDC power plants and additionally to expand specific transmission lines of the transmission grid. Another barrier of the overlay grid is that single regions can be stressed by a large number of power kilometres and do not profit much from such a grid (e.g. model region **SW**). For point-to-point CSP-HVDC power plants also high power kilometre can occur for some regions. In this case CSP-HVDC can be bundled and may lead to a lower impact than a spatial extend of an overlay grid. CSP-HVDC offers also a specific financial and procedure participation of affected persons due to its project specific characteristic [13]. Each point-to-point CSP-HVDC power plant can be handled as a single project with precise business case possibility [13]. This may also be the case for certain grid expansion corridors of a specific overlay grid. The application of an overlay grid together with CSP-HVDC is essential to use the spatial flexibility of a proportionate overlay grid and a suitable share of renewable dispatchable energy of CSP-HVDC. Their synergetic combination can reduce infrastructural requirements and allow an easier system operation.

3.3 Results Part 3

3.3.1 *System cost uncertainty in Germany*

For the analysis of Germany as an isolated model region with a 100% renewable energy system in the year 2050 six cost sensitivity scenarios are applied showing the annual system cost bandwidth in Figure 15. The cost sensitivities are a combination of technological cost assumptions: maximum cost, medium cost and minimal cost with the two grid and transmission line infrastructures overhead lines and underground cables. Nine scenarios (bars in Figure 15) are based on a share of dispatchable and fluctuating renewable energies. This is shown in Figure 15 on the x-axis with the shares of dispatchable_fluctuating energy in relation to gross electricity consumption. A domestic dispatchable renewable energy share of more than 20% is seen as unrealistic due to missing domestic resources. Thus higher dispatchable renewable energy share include CSP-HVDC from the MENA region. The colours in Figure 15 show in green the minimal bandwidth and in red the maximum bandwidth of system cost as uncertainty.

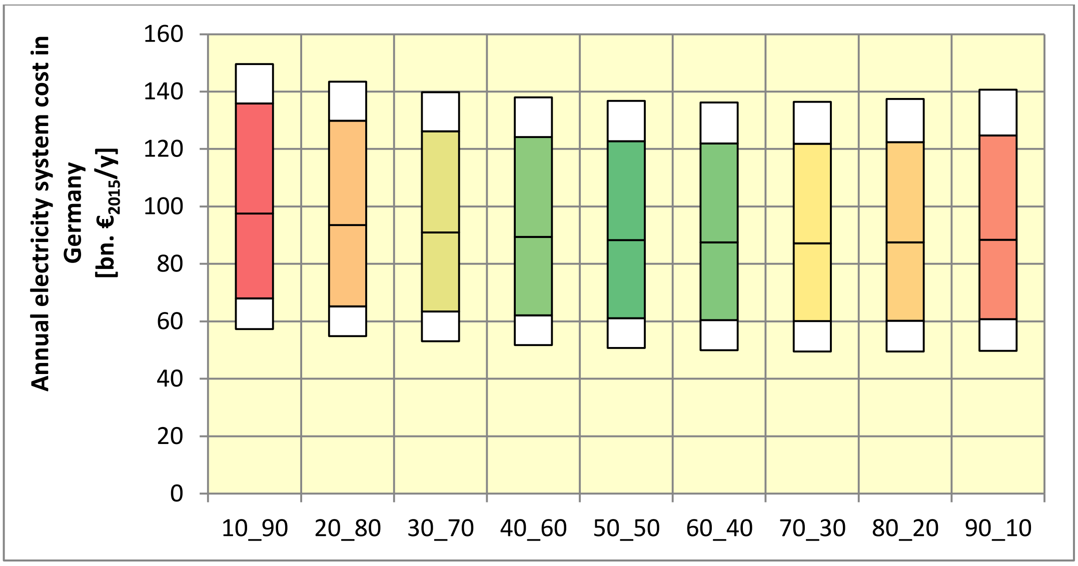

Figure 15: Bandwidth of annual system cost in Germany for the year 2050 with 100% renewable energy [14].

Annual system cost includes cost of annual operation and maintenance (O&M), fuel cost and annuity capital expenditures. System cost uncertainty referred to minimal median value in Figure 15 is -46% to +59%. A well-balanced renewable energy mix of dispatchable and fluctuating energy can reduce system cost uncertainty up to 7% of maximum system cost bandwidth. This equates to less system cost deviation of 6 bn. €/y. However, system cost minimum does not distinguish strongly and system cost bandwidths overlap in all scenarios consequently as a result of these system cost bandwidths. Thus, system cost doesn't play a major role in deciding between more fluctuating or more dispatchable energy shares from today's point of view. However, when calculating with determined and well known cost (no bandwidths), the right mixture of fluctuating and dispatchable share might save up to double-digit billions of € per year.

4 Summary - the value of a dispatchable CSP transfer

This section summarizes the major findings for the value of CSP-HVDC and gives an outlook of further research demand.

Table 8 highlights the qualitative comparison of the used evaluation criteria. It shows higher (-), lower (+) or equal (0) values for two energy systems neglecting CSP-HVDC and integrating CSP-HVDC. This qualitative comparison targets to evidence system advantages and disadvantages. Table 8 reveals with the background colours a final evaluation of the indicators for the two energy systems. The evaluation of the indicators can depend on an integration of CSP-HVDC per se or on the share of CSP-HVDC and model region. The latter concerns system cost uncertainty and total power kilometre.

Table 8: Comparison of evaluation criteria of two energy systems in EUMENA without and with CSP-HVDC

Evaluation criteria	Indicators (higher - / lower + / equal 0)	No CSP-HVDC	With CSP-HVDC
Cost	System cost	0	0
	System cost uncertainty	-	- / +[a]
Infrastructure	Power plant capacity	-	+
	Electrical storage capacity	-	+
	Total power km*	- / +	- / +[a]
	Nodal grid power km	-	+
	CSP P2P power km	+	-
Operational behaviour	Grid stress	-	+
	Curtailment	-	+
Emission	CO_2 emission	0	0 / +[b]

Legend of indicator evaluation

	negative		balanced		positive		neutral

* Total power kilometre is defined as capacity of a power line over distance. This includes the overlay grid, P2P and nodal grid.

[a] Evaluation is positive because the indicator can show a lower impact with CSP-HVDC having more options for action. The indicator strongly depends on the share of CSP-HVDC and the model region.

[b] Evaluation is neutral because the influence of the lower indicator is insignificant on the entire energy system. A lower indicator can be achieved depending on the model region and allows a higher degree of freedom and options for action in a model region.

Cost:

- System cost:
  A minimization of system cost is a major objective for an energy system. As shown in Figure 11, system cost differences between two scenarios can be small. Thus, comparing a system without and with CSP-HVDC, system cost differs not much. Due to high cost uncertainty for a future energy system in the year 2050 (up to ±50% of medium system cost) a statement of future system cost is not robust. Therefore the indicator is evaluated as neutral to avoid a wrong evaluation.
- System cost uncertainty:
  System cost bandwidths represent system cost uncertainty. Such bandwidths are analysed for Germany with different shares of renewable and dispatchable energy shares in Figure 15. A well-balanced mix of dispatchable and fluctuating energies to about equal shares can reduce system cost uncertainty up to 7% of maximum system cost bandwidth. Such a mix includes CSP-HVDC as supplementing technology to achieve an adequate dispatchable share. However, a high share of CSP-HVDC can also increase system cost uncertainty. Without CSP-HVDC a minimum system cost uncertainty can't be reached for Germany in a complete renewable energy system. Other dispatchable renewable energies are limited in their resource potential and can't contribute sufficiently to a suitable renewable dispatchable energy share. Thus, CSP-HVDC reduces system cost uncertainty. The indicator system cost uncertainty is therefore considered to be positive for a system that includes an adequate share of CSP-HVDC and negative if this technology option is missing.

Infrastructure:

- Power plant capacity and electrical storage capacity:
  The capacities of energy supply and flexibility options such as electrical storage represent an environmental indicator for the energy system. Higher capacities can

have a higher environmental impact. Hence, the assumption of high capacities to low cost needs to be scrutinised. Comparing the scenarios with and without CSP-HVDC, the capacity with CSP-HVDC is lower. Avoiding high supply peaks of fluctuating energies, CSP-HVDC can complement such technologies and avoids a high capacity expansion. Also its firm capacity can reduce back-up capacity in EU, if firm capacity abroad is politically accepted as such.

- Total power kilometre:

  As shown in Figure 10 a transmission of electricity over distance is a cost-efficient flexibility option. The use of an overlay grid, point-to-point transmission lines and the expansion of nodal grid reduces cost, curtailment, power plant and storage capacity expansion. However, high amounts of power kilometre are hard to implement due to low social acceptance [27]. The consequences of a reduced power kilometre expansion are higher values of evaluation criteria such as power plant and storage capacities and curtailment. Using high shares of CSP-HVDC increases total power kilometre. An adequate share of CSP-HVDC leads to lower total power kilometre for some model regions (see Figure 14). This increases the impact with respect to other evaluation criteria but it still leads to lower evaluation criteria than a scenario without CSP-HVDC. The indicator total power kilometre is therefore considered to be positive due to a higher degree of freedom and more options for action including CSP-HVDC. Without this technology the indicator is evaluated as balanced due to a potential higher but also lower impact for the entire EUMENA region.

- Nodal grid and CSP-HVDC P2P:

  The nodal grid, defined as the combination of transmission and distribution grid inside a region, is expanded in the case of a higher share of fluctuating energy. In other words: the lower the dispatchable share the higher the nodal grid expansion. A scenario that includes CSP-HVDC reduces power kilometre of the nodal grid (see Figure 12). However, as mentioned before, higher shares of CSP-HVDC can increase total power kilometre due to more needed CSP-HVDC P2P power kilometre. Thus, a trade-off arises between nodal grid power kilometre and CSP-HVDC P2P power kilometre. An adequate CSP-HVDC share is therefore essential to reduce total power kilometre.

Operational behaviour:

- Grid stress:

  The operational behaviour of the grid is influenced by the capacity limit of transmission lines. The more often the capacity limit is reached the higher the stress for the grid and the more often is the potential intervention by the transmission system operator. Reaching capacity limits of the transmission lines is analysed by numbers of peaks in the grid. Including CSP-HVDC reduces such peaks up to 29% and therefore the grid stress (see Table 7). Reducing peaks leads to fewer possible bottlenecks in the grid. Consequently, CSP-HVDC allows a better application possibility of the grid.

- Curtailment:
  Managing a high share of curtailment is a major challenge for the operation of the energy system. A higher curtailment means a higher intervention to curtail energy of specific power plant parks. Some small power plants such as decentralised PV are difficult to curtail due to missing switches. An open question is also how such interventions can be executed with the acceptance of the power plant operator. CSP-HVDC can reduce the amount of electrical curtailment of up to 25% compared to the scenario without this technology (depending on CSP-HVDC share and region – see Figure 31). Thus, CSP-HVDC allows an easier system operation.

Emission:

- CO_2 emission
  CO_2 emission is equal in both scenarios for EUMENA. However, the regional CO_2 emission differs. In the scenario with CSP-HVDC, the MENA regions have a higher degree of freedom to emit CO_2 while they would still stay inside the EUMENA carbon emission limit. This means a small advantage of using CO_2 emitting technologies. The EU region can therefore support the MENA region by integrating CSP-HVDC. However, the difference of regional CO_2 emission is small and has a low impact. Thus, the indicator is considered to be neutral.

4.1 Conclusion: the value of CSP-HVDC

The summary of Table 8 shows, that the advantages of an inclusion of CSP-HVDC outweigh the disadvantages regarding the applied evaluation criteria. This leads to the conclusion that CSP-HVDC is useful and promising for the energy system in EUMENA, and in its sub-regions EU, MENA and Germany. Having in mind that CSP-HVDC is conservatively modelled, the outlined advantages are underestimated rather than overrated. Finally, it depends on the share of CSP-HVDC capacity that quantifies the resulting advantages and disadvantages for the energy system.

4.2 Further research demand and application possibility: feasibility study

Further research in the field of applied energy infrastructures should be in the focus to accelerate the energy transition towards low carbon emissions. A major barrier but also a people-uniting chance could be the point-to-point connection of CSP-HVDC in a multinational environment. The most important spark is the human willingness for a specific project implementation. To implement such a system beneficial technology, it needs at first a CSP-HVDC feasibility study and the will to finance such a study. Secondly, it requires the intention from offtakers in the EU to purchase such electricity. Power purchase agreement and guarantees are essential for financial issues [13]. Thirdly, it needs the agreement of a region in MENA to provide suitable land for the CSP-HVDC power plant. Than a convenient HVDC point-to-point transmission pathway must be found including participatory issues. Neglecting other essential details in between which might emerge only in a feasibility study, investors must be found, approvals must be granted and the construction can begin. Open questions remain for a specific implementation of this technology if no interdisciplinary feasibility study e.g. in g*eographical, technical and financial impact, political and framework assessment* is realised [28]. Thus, such a study is essential for a further step benefiting from the multifaceted system advantages of CSP-HVDC. The results of the present paper point out the business case opportunity of a CSP transfer from North Africa and Middle East to Europe due to its valuable systemic use in Europe. This can lead to a beneficial supplier – offtaker relation bringing people closer together through renewable and dispatchable energies.

Acknowledgement

While good research only lives due to critical discussions, I would like to thank Franz Trieb, Tobias Fichter, Massimo Moser, Jürgen Kern, Hans Christian Gils, Yvonne Scholz, Felix Cebulla, Karl-Kiên Cao, Manuel Wetzel and Ben Fuchs for their programming hints and exchange in the field of sustainable energy systems.

Post-print – Please quote as: Hess, D. The value of a dispatchable concentrating solar power transfer from Middle East and North Africa to Europe via point-to-point high voltage direct current lines. Applied Energy, 2018 (accepted)

Symbols

Abbreviations

AC	Alternating current
AUE	Arab Union of Electricity
CCS	Carbon Capture and Storage
CSP	Concentrated Solar Power
CSP-HVDC	Concentrated Solar Power plant combined with a point-to-point high voltage direct current transmission line
DLR	Deutsches Zentrum für Luft- und Raumfahrt – German Aerospace Center
DNI	Direct Normal Irradiance
ENTSO-e	European Network of Transmission System Operators for Electricity
EU	Geographical Europe
EUMENA	Europe, Middle East and North Africa
GDP	Gross Domestic Product
GHI	Global Horizontal Irradiance
HVDC	High voltage direct current
MENA	Middle East and North Africa
NPP	Net primary production
O&M	Operation and Maintenance
OECD	Organisation for Economic Co-operation and Development
OHL	Overhead line
P2G2P	Power-to-Gas-to-Power
P2P	Point-to-point
PEMFC	Proton exchange membrane fuel cell
PV	Photovoltaic
REMix-EnDAT	Renewable Energy Mix - Energy Data Analysis Tool
REMix-OptiMo	Renewable Energy Mix - Energy System Optimization
UGC	Underground cable
UN	United Nation
USA	United States of America
UTC	Universal Time, Coordinated

Parameters

Parameter	Unit	Description
$c_{Emission}$	[k€/GWh]	specific emission cost
c_{Fuel}	[k€/GWh]	specific fuel cost
$c_{O\&M\ Fix}$	[%/y]	specific operation and maintenance fix costs
$c_{O\&M\ Variable}$	[k€/MWh]	specific operation and maintenance variable costs
$c_{specInv}$	[k€/MW]	specific investment cost
$f_{annuity}$	[-]	Annuity factor
$\eta_{generator}$	[%]	Efficiency of the generator
η_{charge}	[%]	Charging efficiency of the storage
$\eta_{discharge}$	[%]	Discharging efficiency of the storage
η_{self}	[%]	Self-discharging rate of the storage
i	[%]	Interest and discount rate
$P_{existCap}$	[GW_{el}]	Capacity of existing power plants
P_{HVDC}	[GW_{el}]	Capacity of the HVDC transmission line
$P_{PB,\ CSP}$	[GW_{el}]	Capacity of the CSP power block
$P_{SF,\ CSP}$	[GW_{th}]	Capacity of the CSP solar field
$P_{TES,\ CSP}$	[GWh_{th}]	Thermal energy storage capacity of the CSP
$s_{gen}(t)$	[-]	Normalised generation time series of fluctuating energy
SM	[-]	Solar Multiple
Δt	[h]	Calculation time interval
t_y	[y]	Amortization time
t	[h]	Time

Variables

Variable	Unit	Description
$\boldsymbol{C}_{capital}$	[k€/y]	Annual depreciation of capital expenditure
$\boldsymbol{C}_{operation}$	[k€/y]	Operation and maintenance costs
$\boldsymbol{P}_{addedCap}$	[GW_{el}]	Capacity of additional power plants
$\boldsymbol{P}_{gen}(t)$	[GW_{el}]	Power generation
$\boldsymbol{Q}_{addedCap}(t)$	[GW_{th}]	Capacity of model endogenous CSP solar field
$\boldsymbol{Q}_{BUS}(t)$	[GW_{th}]	Thermal output of the CSP co-firing system
$\boldsymbol{Q}_{charge}(t)$	[GW_{th}]	Thermal energy storage input
$\boldsymbol{Q}_{curtail}(t)$	[GW_{th}]	Thermal curtailment of the solar field
$\boldsymbol{Q}_{disharge}(t)$	[GW_{th}]	Thermal energy storage output
$\boldsymbol{Q}_{SF}(t)$	[GW_{th}]	Thermal output of the solar field
$\boldsymbol{U}_{level}(t)$	[GWh_{th}]	Thermal energy storage level

References

[1] S. Pfenninger, P. Gauché, J. Lilliestam, K. Damerau, F. Wagner and A. Patt, “Potential for concentrating solar power to provide baseload and dispatchable power,” *Nature Climate Change,* vol. 4, p. 689–692, 2014.

[2] Y. Scholz, RENEWABLE ENERGY BASED ELECTRICITY SUPPLY AT LOW COSTS: DEVELOPMENT OF THE REMIX MODEL AND APPLICATION FOR EUROPE, Stuttgart: University Library of the University of Stuttgart, 2012.

[3] S. Cole, K. Karoui, T. K. Vrana, O. B. Fosso, J.-B. Curis, A.-M. Denis and C.-C. Liu, “A European Supergrid: Present state and future challanges,” Stockholm, 2011.

[4] ABB, “HVDC,” 2017. [Online]. Available: http://new.abb.com/systems/hvdc. [Accessed 06 22 2017].

[5] M. Benasla, T. Allaoui, M. Brahami, M. Denaï and V. K. Sood, “HVDC links between North Africa and Europe: Impacts and benefits on the dynamic performance of the European system,” *Renewable and Sustainable Energy Reviews,* vol. 82, pp. 3981-3991, 2018.

[6] U. Desideri and P. E. Campana, “Analysis and comparison between a concentrating solar and a photovoltaic power plant,” *Applied Energy,* vol. 113, pp. 422-433, 2014.

[7] K. Schaber, F. Steinke and T. Hamacher, “Transmission grid extensions for the integration of variable renewable energies in Europe: Who benefits where?,” *Energy Policy,* vol. 43, pp. 123-135, 2012.

[8] M. Fürsch, S. Hagspiel, C. Jägemann, S. Nagl, D. Lindenberger and E. Tröster, “The role of grid extensions in a cost-efficient transformation of the European electricity system until 2050,” *Applied Energy,* vol. 104, pp. 642-652, 2013.

[9] M. Haller, S. Ludig and N. Bauer, “Decarbonization scenarios for the EU and MENA power system: Considering spatial distribution and short term dynamics of renewable generation,” *Energy Policy,* vol. 47, pp. 282-290, 2012.

[10] H. Gils, “Economic Potential for Future Demand Response in Germany – Modelling Approach and Case Study. doi:10.1016/j.apenergy.2015.10.083,” *Applied Energy,* vol. 162, p. 401–415, 2016.

[11] R. Domínguez, A. Conejo and M. Carrión, “Operation of a fully renewable electric energy system with CSP plants,” *Applied Energy,* vol. 119, pp. 417-430, 2014.

[12] DLR, “TRANS-CSP,” 2006.

[13] D. Hess, FERNÜBERTRAGUNG REGELBARER SOLARENERGIE VON NORDAFRIKA NACH MITTELEUROPA, Stuttgart: University Library of the University of Stuttgart, 2013.

[14] D. Hess, M. Wetzel and K.-K. Cao, “Representing node-internal transmission and distribution grids in energy system models,” *Renewable Energy,* 2017.

[15] D. Hess, “The Value of Concentrating Solar Power for a Sustainable Electricity Supply in Europe, Middle East and North Africa,” 2018.

[16] D. Stetter, ENHANCEMENT OF THE REMIX ENERGY SYSTEM MODEL: GLOBAL RENEWABLE ENERGY POTENTIALS, OPTIMIZED POWER PLANT SITING AND SCENARIO VALIDATION, Stuttgart: University Library of the University of Stuttgart, 2012.

[17] H. C. Gils, Y. Scholz, T. Pregger, D. Luca de Tena and D. Heide, “Integrated modelling of variable renewable energy-based power supply in Europe,” *Energy,* vol. 123, p. 173–188, 2017.

[18] J. Rogelj, G. Luderer, R. C. Pietzcker, E. Kriegler, M. Schaeffer, V. Krey and K. Riahi, “Energy system transformations for limiting end-of-century warming to below 1.5 °C,” *Nature Climate Change,* vol. 5, p. 519–527, 2015.

[19] G. Knies and A. Bennouna, “Nordafrikanisch - Europäischer Solarenergie Verbund. Workshop des Hamburger Klimaschutz-Fonds HKF am 9.4. 1997 an der TU Hamburg Harburg,” 1997.

[20] United Nations, “World Population Prospects: The 2015 Revision,” 2015.

[21] DLR, “Med-CSP,” 2005.

[22] D. Hess, “The empirical probability of integrating CSP and its cost optimal configuration in a low carbon energy system of EUMENA,” *Solar Energy,* 2018.

[23] S. S. Russian Federal State, “All-Russian Population Census,” 2010.

[24] T. Fichter, Long-term Capacity Expansion Planning with Variable Renewable Energies - Enhancement of the REMix Energy System Modelling Framework, Stuttgart: Universität Stuttgart, 2017.

[25] F. Trieb, C. Schillings, T. Pregger and M. O'Sullivan, "Solar electricity imports from the Middle East and North Africa to Europe," *Energy Policy,* vol. 42, 2012.

[26] N. May, Ökobilanz eines Solarstromtransfers von Nordafrika nach Europa, 2005.

[27] A. Steinbach, "Barriers and solutions for expansion of electricity grids - the German experience," *Energy Policy,* vol. 63, pp. 224-229, 2013.

[28] BETTER, "Bringing Europe and Third countries closer together through renewable Energies," 2015.

[29] IEA, "Internatioanl Energy Agency Statistics," 2017. [Online]. Available: http://www.iea.org/statistics/. [Accessed 14 02 2015].

[30] F. Trieb and U. Klann, "Modeling the Future Electricity Demand of Europe, Middle East and North Africa," Stuttgart, 2006.

[31] IPCC, "Mitigation of Climate Change," 2014.

[32] IPCC, "Mitigation of Climate Change," 2014.

[33] IIASA, "Shared Socioeconomic Pathways Database," 03 2013. [Online]. [Accessed 03 08 2015].

[34] L. Gruber, "Synthese globaler, elektrischer Lastganglinien," Berlin, 2012.

[35] G. Pleßmann, M. Erdmann, M. Hlusiak and C. Breyer, "Global Energy Storage Demand for a 100% Renewable Electricity Supply," *Energy Procedia,* vol. 46, pp. 22-31, 2014.

[36] S. Kühnel, Investigation of the variability of solar and wind electricity generation potentials in Europe and North Africa, Oldenburg: Karl von Ossietzky University, 2013.

[37] H. Gils, "Assessment of the theoretical demand response potential in Europe. doi:10.1016/j.energy.2014.02.019," *Energy,* vol. 67, pp. 1-18, 2014.

[38] G.-G. Marcos and L.-A. Roberto, "Assessment of the European potential for pumped hydropower energy storage: A GIS-based assessment of pumped hydropower storage

potential," 2013.

[39] A. Moser, "Unterstützung der Energiewende in Deutschland durch einen Pumpspeicherausbau," 2014.

[40] FIAS, 2017. [Online]. Available: https://github.com/FRESNA/powerplantmatching. [Accessed 03 05 2016].

[41] R. Jung, S. Röhling, N. Ochmann, S. Rogge, R. Schellschmidt, R. Schulz and T. Thielemann, "Abschätzung des technischen Potenzials der geothermischen Stromerzeugung und der geothermischen Kraft-Wärmekopplung (KWK) in Deutschland," 2002.

[42] M. Tum, I. M. Kurt P. Günther, G. Kindermann and E. Schmid, "Sustainable Bioenergy Potentials for Europe and the Globe," *Geoinformatics & Geostatistics: An Overview,* pp. 1-10, 2013.

[43] Mai et al., "COST AND PERFORMANCE DATA FOR POWER GENERATION TECHNOLOGIES," 2012.

[44] IEA, "PV Roadmap," 2010.

[45] E. P. Agency, "Data from Integrated Power Model (IPM), ICF International," 2010.

[46] Department of Energy, "Estimate Value 2030," 2011.

[47] IEA, "Data from Market Allocation (MARKAL) model, International Energy Agency and Brookhaven National Laboratory," 2009.

[48] OPENEI NREL, "The data below was downloaded from the Transparent Cost Database at http://en.openei.org/apps/TCDB/".

[49] Environmental Protection Agency, *Data from Integrated Power Model (IPM), ICF International.,* 2010.

[50] IRENA, "IRENA Hydro Power," 2012. [Online]. Available: http://www.irena.org/documentdownloads/publications/re_technologies_cost_analysis-hydropower.pdf.

[51] J. Nitsch and et al., "Long-term scenarios and strategies for the deployment of

renewable energies in Germany in view of European and global developments," 2012.

[52] Pregger, "Vergleichende Bewertung der Integration einer zentralen versus einer dezentralen Wasserstofferzeugung in die zukünftige Stromversorgung Deutschlands," 2015.

[53] U. Albrecht and et al., "Analyse der Kosten erneuerbarer Gase," BWE, 2013.

[54] D. Fürstenwerth and et al., "Stromspeicher in der Energiewende," Agora, 2014.

[55] J. Nitsch and T. Pregger, "Kostenbilanz des Ausbaus erneuerbarer Energien in der Stromerzeugung bei unterschiedlichen Preisbildungen am Strommarkt," *Vierteljahrshefte zur Wirtschaftsföderung,* vol. 82, pp. 45-59, 2013.

[56] E. S. Rubin, C. Chen and A. B. Rao, "Cost and performance of fossil fuel power plants with CO2 capture and storage," *Energy Policy,* vol. 35, p. 4444–4454, 2007.

[57] European Commission, "Press releases database," 08 10 2014. [Online]. Available: http://europa.eu/rapid/press-release_IP-14-1093_de.htm. [Accessed 20 03 2015].

[58] G. v. Goerne, CO2-Abscheidung und -Lagerung(CCS) in Deutschland, Germanwatch Nord-Süd Initiative e.V., 2009.

[59] H. Brakelmann, "Netzverstärkungs-Trassen zur Übertragung von Windenergie: Freileitung oder Kabel ?," Rheinberg, 2004.

[60] L. Neij, "Cost development of future technologies for power generation—A study based on experience curves and complementary bottom-up assessments," *Energy Policy 36,* p. 2200– 2211, 2008.

[61] CSP-Today, "CSP-Today," 15 02 2016. [Online]. Available: http://www.csptoday.com/.

[62] P. Viehbahn and et al., "EU-NEEDS scenario pesimistic," 2008.

[63] Greenpeace, "scenario optimistic," 2009.

5 Appendix

5.1 Comparison of point-to-point interconnection, meshed overlay grid and their combination

Table 9a and b highlight the advantages and disadvantages of the point-to-point and overlay grid infrastructure. Table 9c indicates their combination. Good planning ability and high spatial flexibility of the energy supply might be the optimum of an energy transmission infrastructure. However, transmission line infrastructures are difficult to be implemented already nationally due to low social acceptance [27]. Thus, the effort in building new transmission capacity should remain low, using as many advantages of point-to-point and overlay grid infrastructure as possible which is only feasible of course in a combination.

Table 9: Overview of point-to-point transmission lines and meshed overlay grid

<table>
<tr><th>Relative merits of transmission line and grid topology</th><th>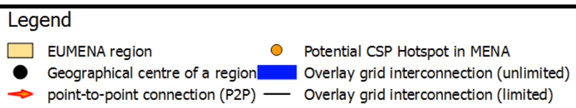
</th></tr>
<tr><td>Point-to-point transmission lines

Advantage
Projectable with specific producers and offtakers thus a clear business case is possible [28].
Bundling of transmission lines can allow common infrastructure corridors.
Disadvantage
Transmission line expansion is needed inside a multi-national structure.</td><td>a
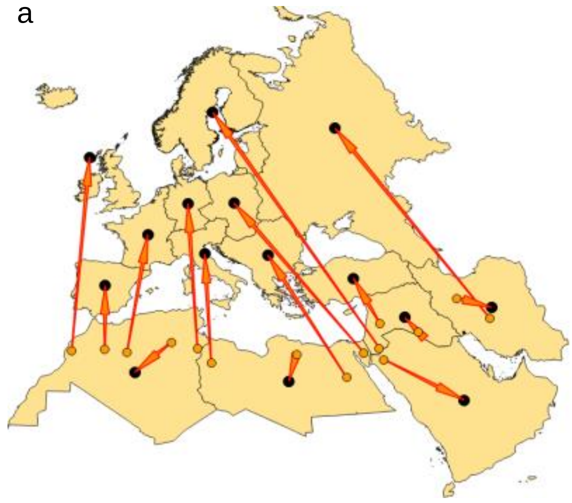</td></tr>
<tr><td>Meshed overlay grid

Advantage [3]
Can increase the overall reliability.
Can balance renewable energy due to a large spatial expansion.
International trade possibility.
Disadvantage
Huge planning effort over a large area with a multitude of different authorities.
Unclear financing and operation.</td><td>b
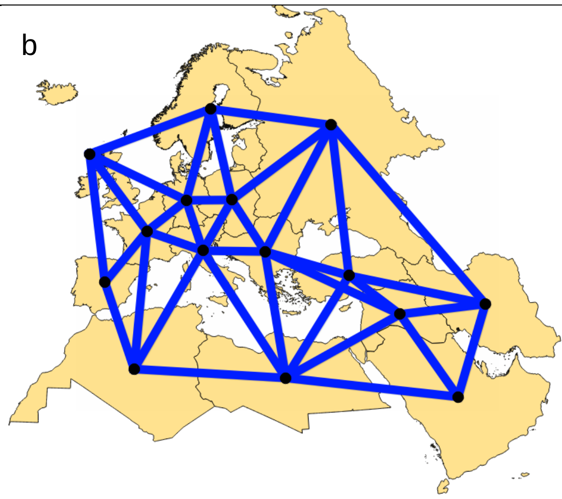</td></tr>
<tr><td>Expansion of existing grid and meshed overlay grid with point-to-point transmission lines

Advantage
Combination of limited overlay grid (similar to existing transmission grid) and focussed use of dispatchable renewable energy.
Disadvantage
New grid, existing grid and single transmission line expansion is needed.</td><td>c
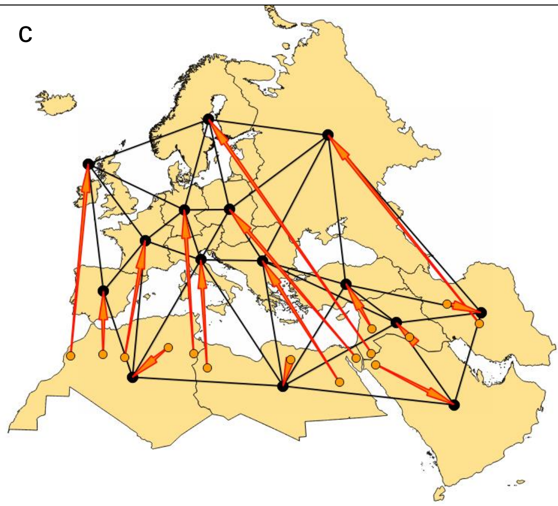</td></tr>
</table>

5.2 Basic modelling assumptions

5.2.1 *Supply technologies*

The REMix model includes weather dependent technologies such as photovoltaic, wind onshore, wind offshore and hydro run-of-river so-called fluctuating renewable energies and non-weather dependent technologies such as biomass, geothermal energy, nuclear, gas, coal fired power plants (also CCS) and CSP with co-firing so-called dispatchable energies. Biomass, geothermal and CSP with thermal energy storage and co-firing are defined as renewable dispatchable technologies. Dispatchable energies can provide electricity according to the demand and offer firm capacity. The electricity generating renewable technologies applied in the thesis are listed in Table 10. These technologies are available today and they are functioning. Contrarily, technologies with a low technological readiness level such as nuclear fusion or a hydrogen turbine are not considered. This allows a pragmatic and robust energy system analysis without speculation of technological breakthroughs from today's point of view. Non-renewable technologies such as nuclear, gas, coal fired power plants (also CCS) are characterised in Table 20 on page 75. Defining the characteristic of a technology, a representative example out of a technology group is selected, but not the whole bandwidth of all specific occurrences of one technology is examined. The examples are representative for the general characteristic of a chosen technology. However, a simplification makes sense comparing only the technology groups in competition to each other. Other applied technologies defined as flexibility options such as electrical storages and the electrical grid. Potentials of pump storage, hydro run-of-river, hydro reservoir, geothermal energy, solid biomass and CSP are limited and are made available in the appendix Table 12.

Table 10: Classification and characteristic of used renewable energies for electricity generation based on [2] – hydro reservoir is considered neither as fluctuating nor as dispatchable but as long term storage with additional natural inflow.

Technology class of electricity generating power plants		**Characteristics**	**Range of validity**
Fluctuating renewable energies	Photovoltaic	Silicon cells with a module efficiency of 18%	Standard test conditions: 25 °C module temperature, 1000 W/m^2 irradiance
Fluctuating renewable energies	Wind Onshore	Rotor diameter: 130 m Hub height: 132 m	Start-up wind speed: 2 m/s, nominal power output is reached at 12 m/s. Cut-off was set to start at 25 m/s and to end at 35 m/s.
Fluctuating renewable energies	Wind Offshore	Rotor diameter: 140 m Hub height: 192 m	
Fluctuating renewable energies	Hydro run-of-river (here fluctuating because of fluctuating water level and no co-firing option)	No power plant model – analysis is based on empirical time series	Power plants in operation, annual generation and generation potentials in Germany
Dispatchable renewable energies (with co-firing option)	Biomass	Power plant with steam turbine - 35% electric efficiency - using forest wood, waste wood, straw and energy crops	Domestic share of net primary production potential, yields and competing use scenarios per country for forestry, agriculture and other sectors - agricultural statistics.
Dispatchable renewable energies (with co-firing option)	Geothermal power	Enhanced geothermal system (EGS)	Depth range 2000 - 5000 m
Dispatchable renewable energies (with co-firing option)	Concentrating Solar power	Parabolic trough power plant with molten salt storage - 37% power block efficiency and 95% storage efficiency -	Reference irradiance - direct normal irradiance (DNI) - with 800 W/m^2, tracking the sun along the north south axis

Other characteristic of power plant and storage are available with technological an economic data in Table 18 to Table 22.

5.2.2 *Demand model*

The analysis considers only the electricity demand. However, the demand model includes an electricity share of heat and mobility. The occurring electricity demand of these two sectors is added to the conventional electricity demand. In the following the assumptions of the demand until the year 2050 are explained showing the data that build the basis of the assumption in the demand model. The historical data of electricity, heat and mobility in the used model start in the year 2010 and are taken form IEA database [29].

- Electricity: net electricity demand (electricity, final consumption)
- Heat: residential and commercial heat demand (from coal, oil and gas)
- Mobility: transport demand (from oil)

The development of the electricity sector is derived from the GDP according to DLR [30]. This reference uses a scenario for the development of the GDP per capita growth rate. The used GDP per capita growth rate in the scenario “closing the gap” assumes to reduce the difference of GDP per capita of a given country to 50% compared with the GDP per capita of the USA in the year 2050. Population data are taken from the UN medium scenario [20]. For the development of the electricity share of the heat sector a 60% electricity share of global buildings final energy demand until 2050 is used and a demand reduction per capita and year (2010 to 2050) of 0.65% in OECD, 0.39% in Middle East and Africa and 0.28% in Eastern Europe and Russia is assumed [31]. The conversion factor using final energy of heat from oil, gas or coal is 90%. For the development of the electricity share of the mobility sector outgoing from 2020 a 15% electricity share of final energy demand until 2050 is used and a demand reduction per capita and year (2010 to 2050) of 1.08% in OECD, -0.45% in Middle East and Africa and -0.82% in reforming countries is assumed [32], [33]. The conversion factor using final energy from oil for mobility is 30%. For heat and mobility there is still a higher share of carbon resource than in the electricity sector in 2050. However, the assumption considers low carbon emission trying to reach the 2°C target [18].

The resulting electricity demand in Table 11 of heat and mobility is added to the electrical load curve with the same profile because today’s load curve already includes heat and mobility shares. The hourly profile of the electrical load curve is taken from ENTSO-e in 2006, Arab Union of Electricity (AUE) in 2012 and a synthetic load profile from [34], [35] and thus represent historical demand curve. It is assumed that these load curves do not have another characteristic than in the year 2050.

Table 11: Annual electrical demand of electricity, heat and mobility sector in 2010 and 2050

Model region	**Electricity demand [TWh]**		**Electrical heat demand [TWh]***	**Electrical mobility demand [TWh]***	**Total electrical demand [TWh]**	
year	**2010**	**2050**	**2050**	**2050**	**2010**	**2050**
G	532	510	173	22	532	706
N	382	541	13	17	382	571
E	235	337	82	11	235	429
S	436	522	141	27	436	689
W	641	673	205	42	641	920
NW	370	552	201	32	370	785
NE	608	839	170	27	608	1037
SE	195	298	15	8	195	321
NAE	151	1127	19	31	151	1178
NAW	71	582	74	19	71	674
SW	295	315	9	18	295	342
T	175	509	90	14	175	613
MES	150	796	99	56	150	950
I	186	484	362	28	186	874
ME	393	869	18	87	393	974
Sum	**4819**	**8953**	**1672**	**439**	**4819**	**11064**

*Additional electrical heat and mobility demand are assumed to be 0 in the year 2010.

The rising electrical demand in EUMENA, which more than doubles from 4819 TWh in 2010 to 11064 TWh in 2050, leads to a capacity expansion and higher demand of resources. Thus, in Europe dispatchable renewable energies such as biomass and geothermal energy can reach their techno-economic limit. Solving this lack, Wind, PV, storage and CSP inside Europe and from MENA can provide renewable energy. It can be expected that a rising electrical demand may lead to a rising demand of renewable dispatchable energy and therefore to a rising demand of a transfer of CSP generated electricity from MENA to Europe.

5.2.3 *Technological time series and electrical load curve*

The time series of CSP, photovoltaic, wind onshore, wind offshore, hydro run-of-river power plants and hydro reservoir natural inflow are country-wide averages calculated with REMix-EnDAT based on bottom-up power plant models (see Table 10) [2], [16]. This calculation includes exclusion areas for renewable energies which define with technology parameters the potential of each renewable energy technology. For each grid box, the approach yields hourly power generation based on technology parameters and resource availability. The hourly time series are available of the years 1984-2004 on global level (resolution 0.045° x

0.045° or ~50km x 50km at equator) [16] and of the years 2006 - today on European level (resolution 0.083° x 0.083°, ~10km x 10km) [2]. For the analysis a typical meteorological year is considered, which is the year 2006 in Europe [2] and the year 2002 in MENA [16]. Two different years can be chosen due to relative low meteorological differences. On European level the output of the time series deviate in the available years of about 15% max. [36]. Possible changes of the renewable resource availability due to climate change are an uncertainty which is not considered in the analysis. Peak load of demand and average resource full load hours of the model regions are available in Table 13. These input data are important for a reproducibility of the results showing key characteristics of annual input values as well as temporal intensity and temporal availability. Figure 16 serves as an example of the electrical load and technological time series of one year for Germany (country average). Here isopleth diagrams are used to illustrate such time series over the day of the year (y-axis) and over the hour of the day series (x-axis). They show in (a) the electrical load as share of peak load, in (b) the normalised availability of generated electricity by PV capacity, in (c) by wind turbines offshore, in (d) by wind turbines onshore, in (e) by hydro run of river power plants, in (f) the normalised availability of natural inflow by hydro reservoir power plants, in (g) by imports of hydro reservoir power plants from Norway, in (h) the normalised availability of generated thermal energy by the solar field of CSP in MENA for Germany and are related to the design point of 800 W/m^2. The hydro reservoir time series are derived from hydro run of river [2]. The CSP time series is an average of selected CSP hotspots.

The temporal profiles reveal the intensity and availability of the demand and the resources. Characteristic for the time series is the time period of regularly and unregularly low and high availability. For example the wind resources show irregular monthly and seasonal lacks (green colour Figure 16c, d) of wind compared to solar resources (black in Figure 16b,h). Solar resources are more periodical available during a year than wind or hydro resources. The availability of the solar resources PV (GHI) is smoother than the scattered resource of CSP (DNI). Comparing PV in Germany and CSP in MENA, it is visible that in winter PV drops in Germany while CSP in MENA stays in its availability nearly constant. Hydro time series are seasonally less fluctuating than wind or solar but not always such intensively available. The load curve shows a peak demand in winter which is typical in northern European regions. All isopleth diagrams of the used model regions refer to one year, start in the lower left corner (0,0) on January 1st and are shown in Figure 16 to Figure 30.

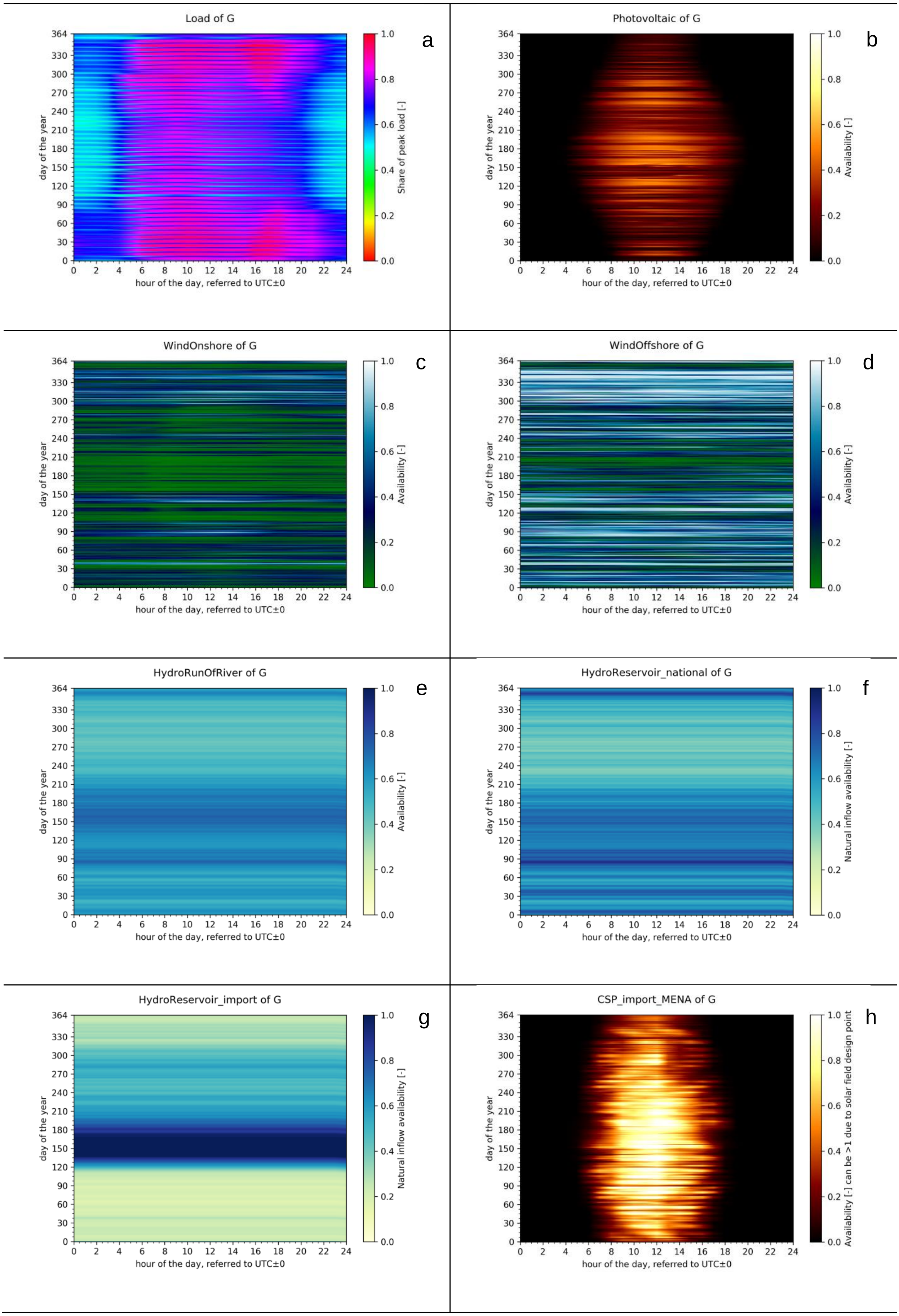

Figure 16: Load and technological time series of model region G

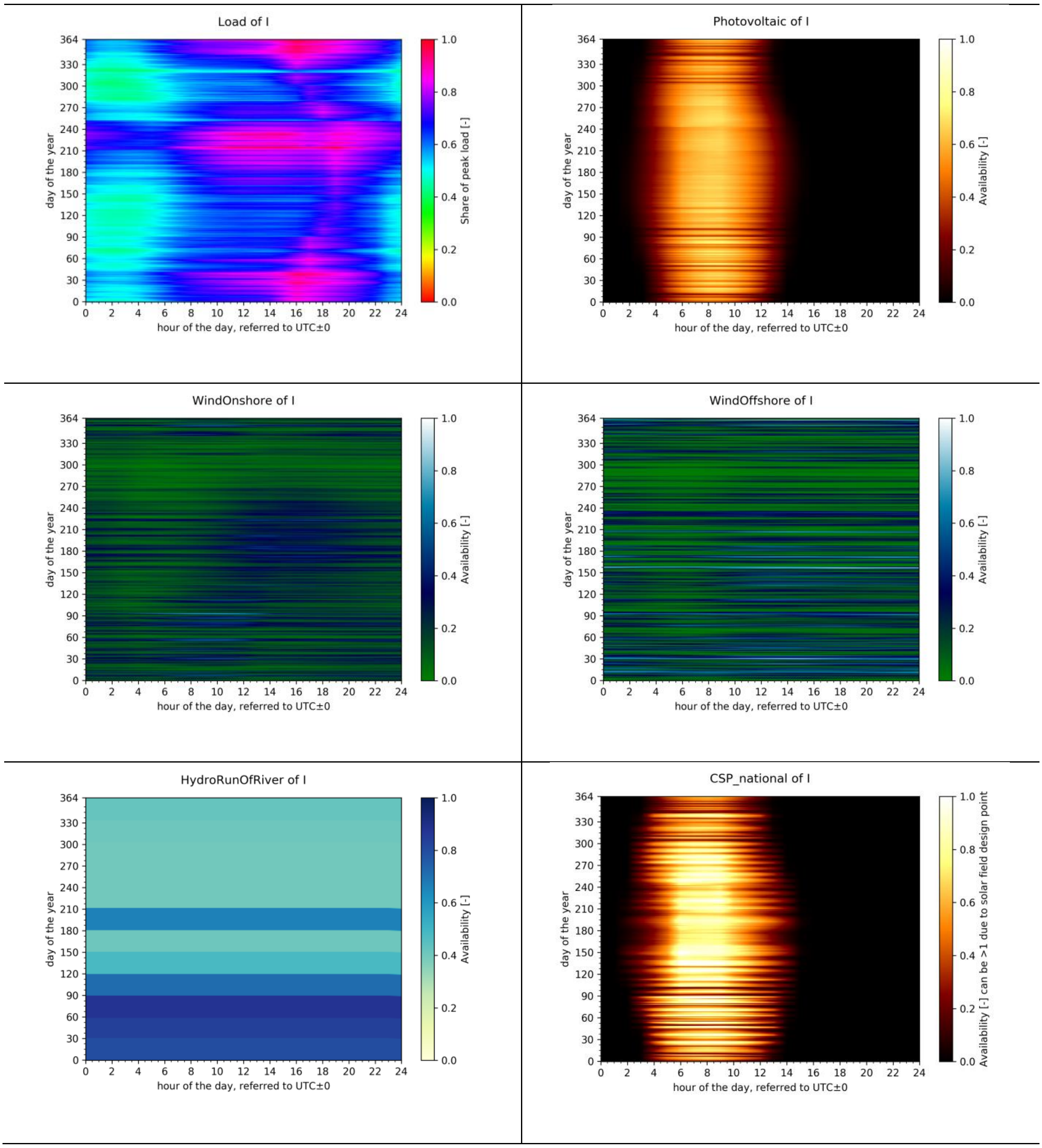

Figure 17: Load and technological time series of model region I

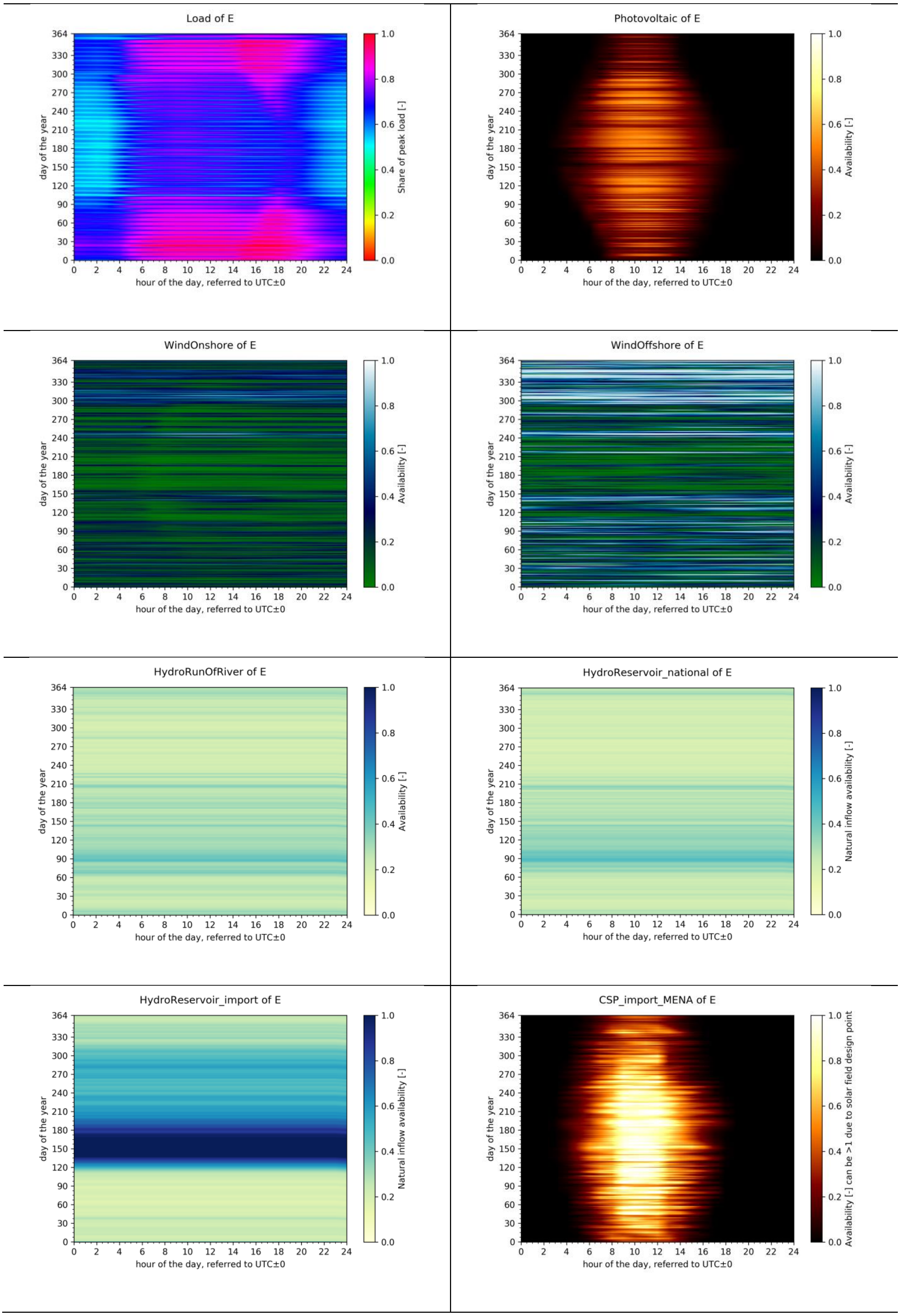

Figure 18: Load and technological time series of model region E

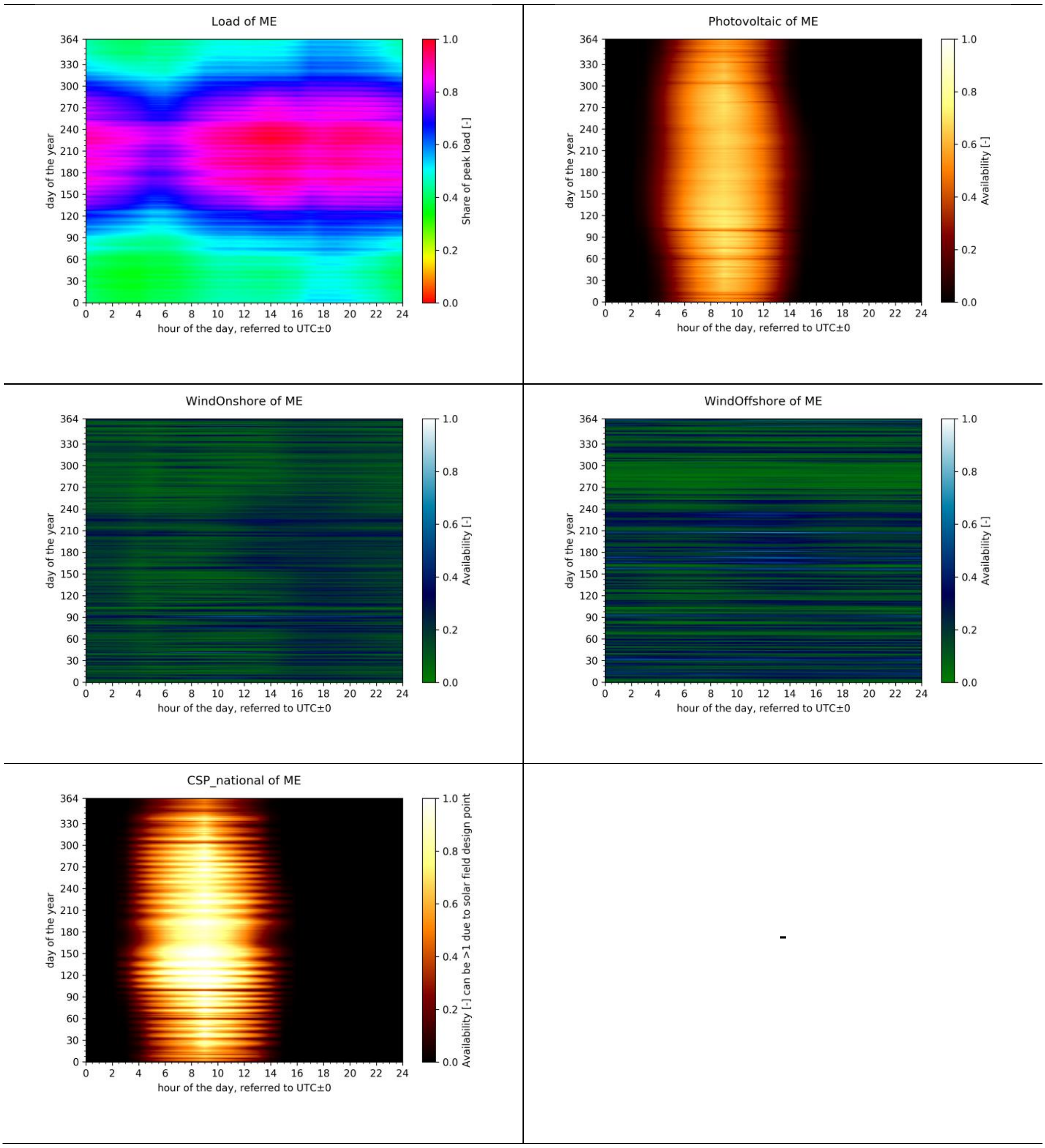

Figure 19: Load and technological time series of model region ME

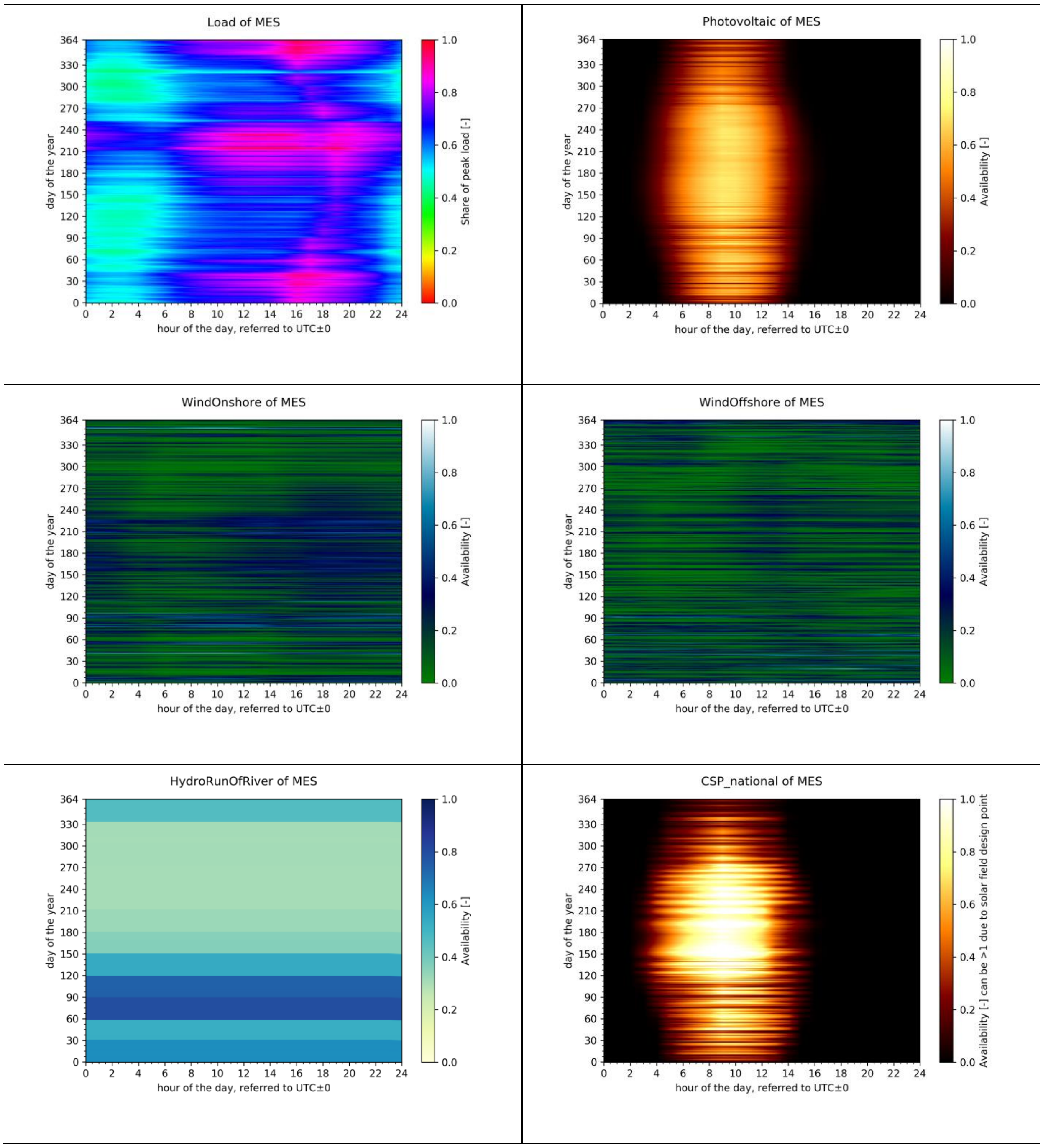

Figure 20: Load and technological time series of model region MES

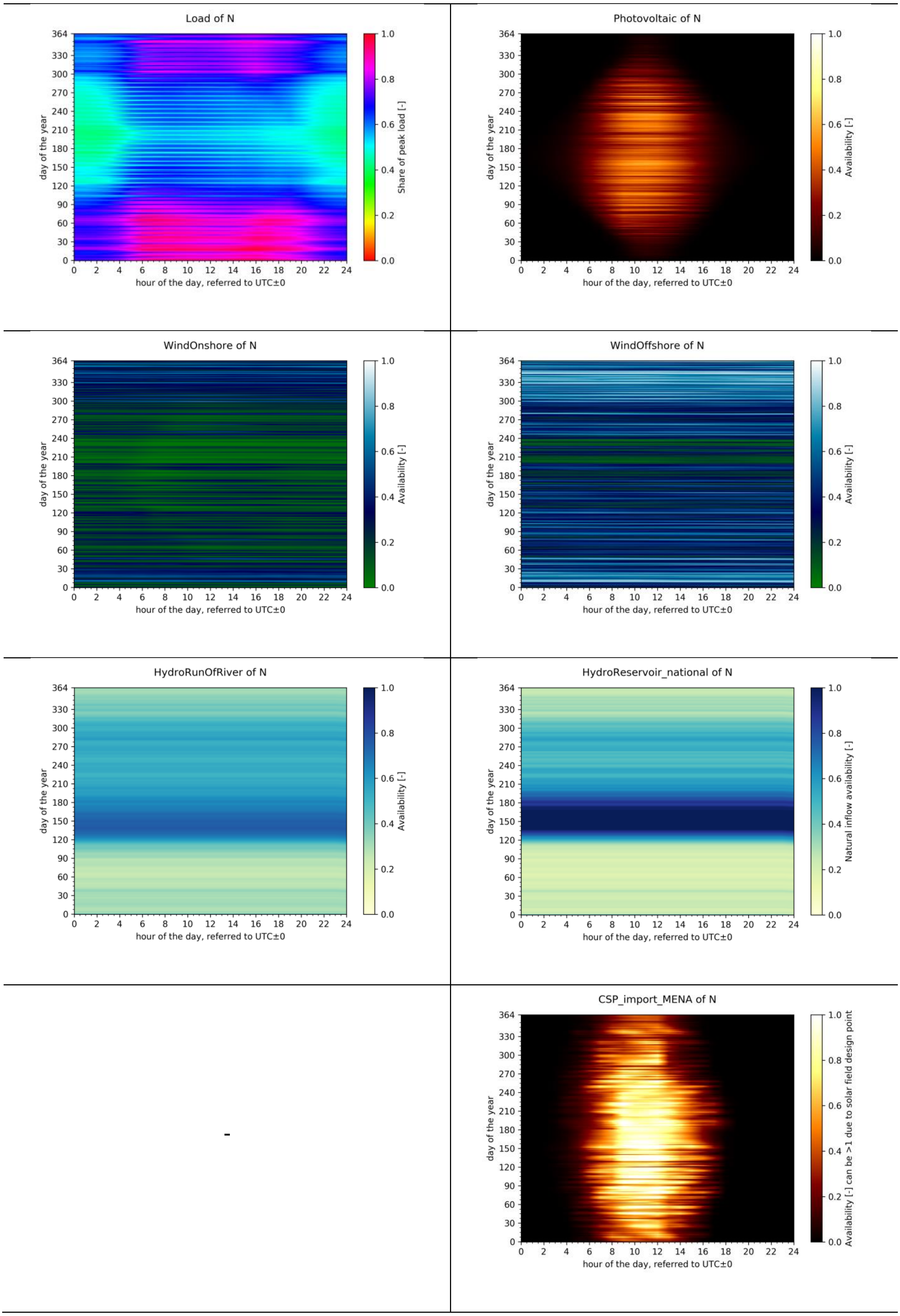

Figure 21: Load and technological time series of model region N

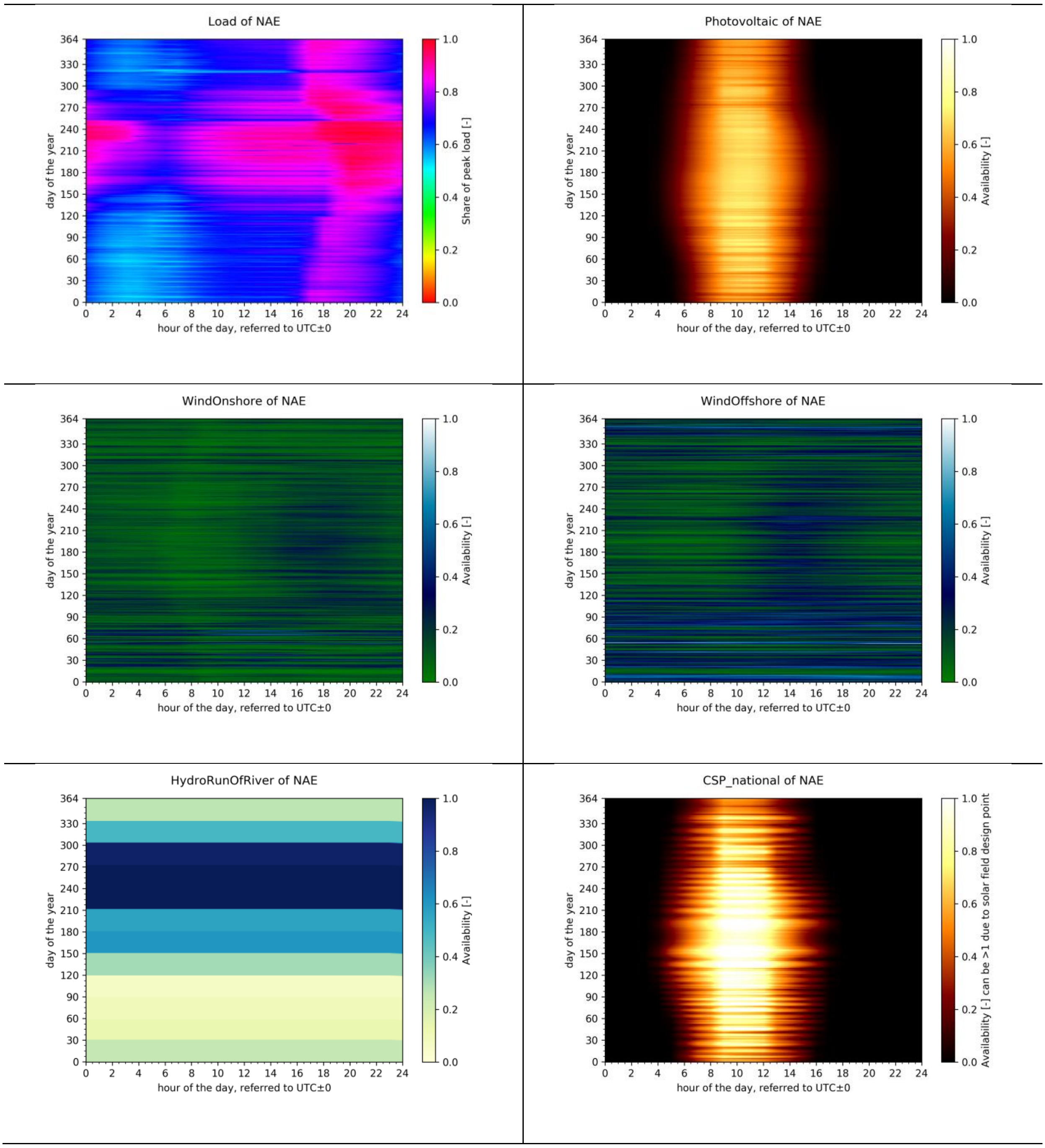

Figure 22: Load and technological time series of model region NAE

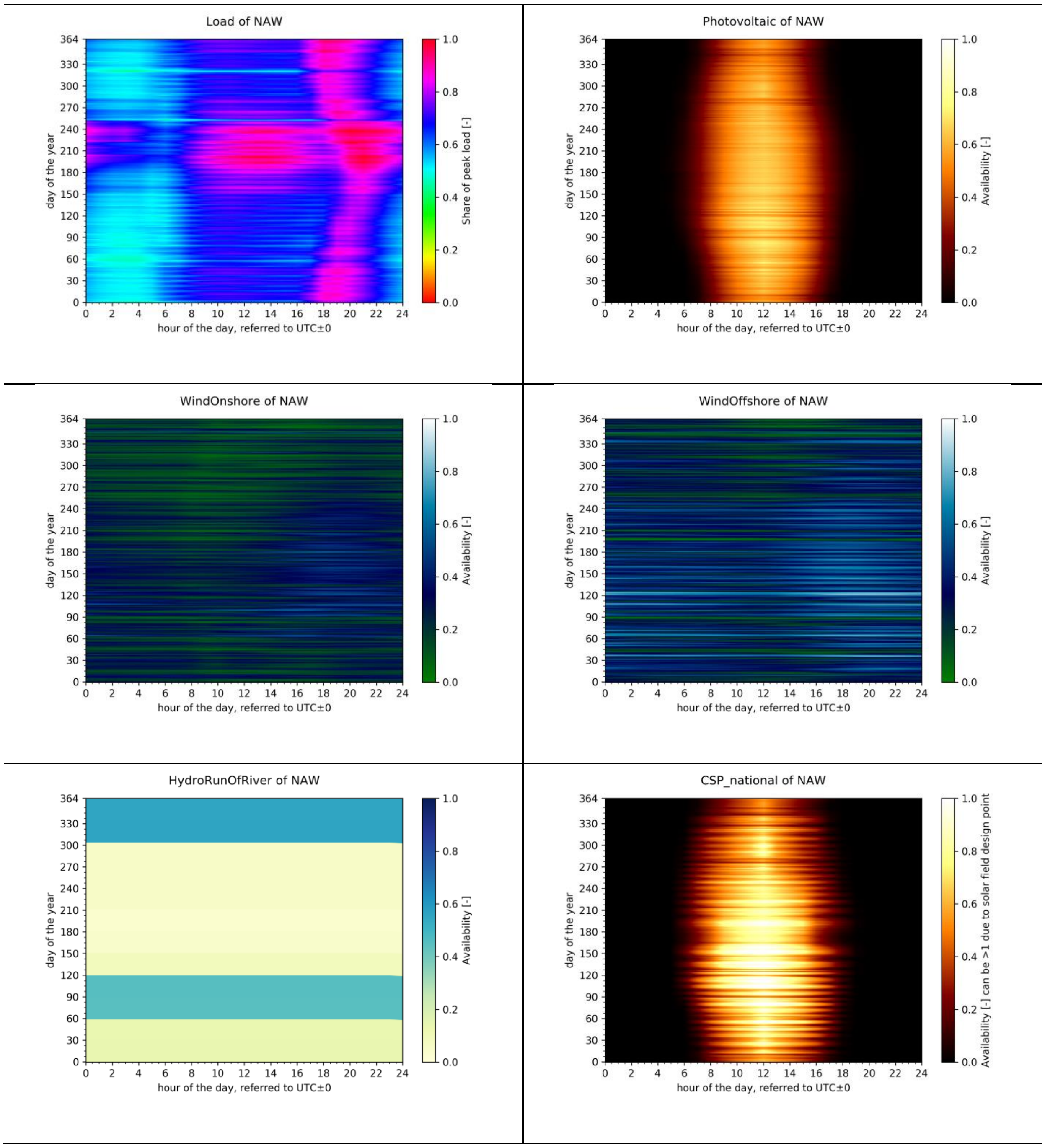

Figure 23: Load and technological time series of model region NAW

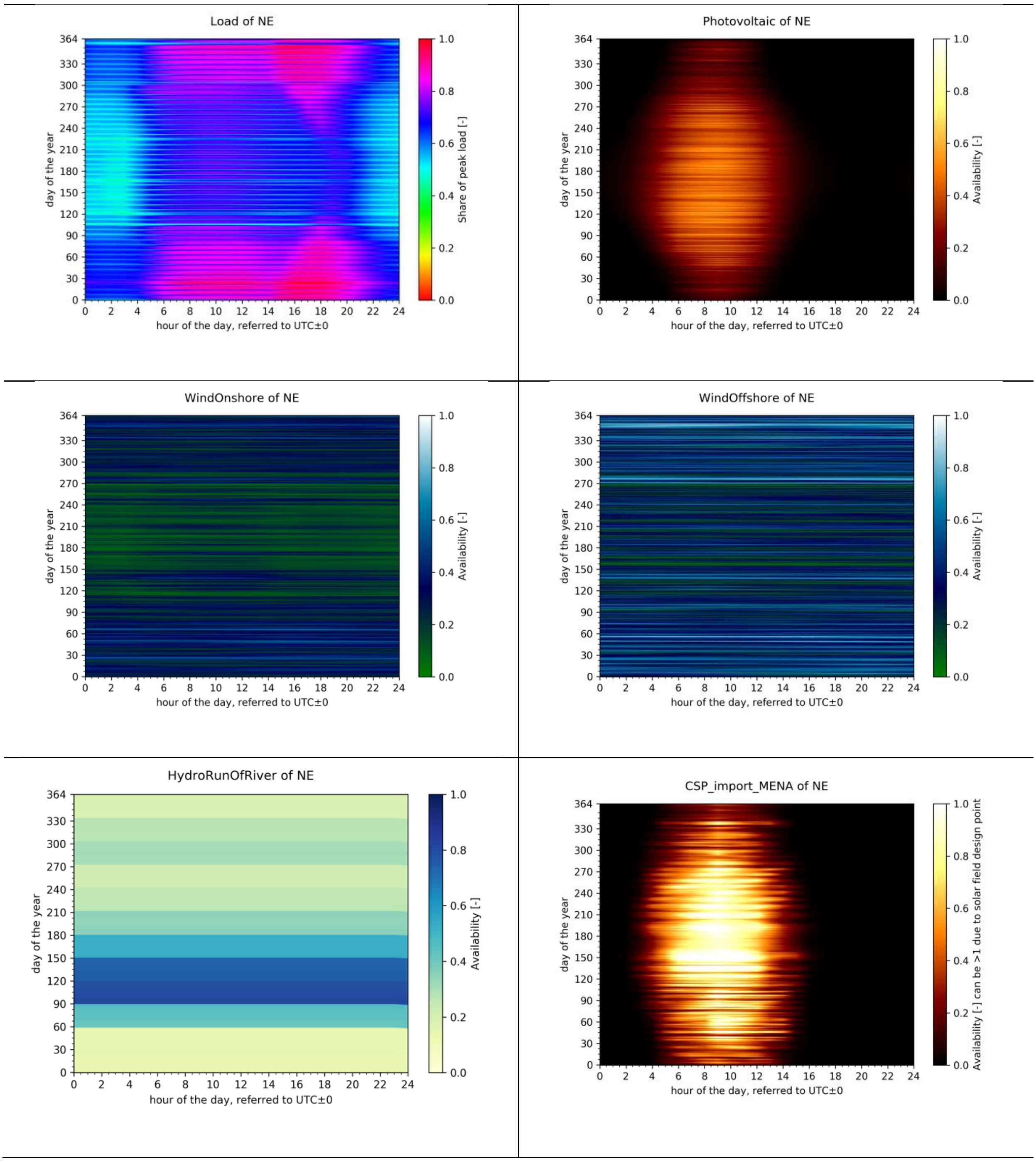

Figure 24: Load and technological time series of model region NE

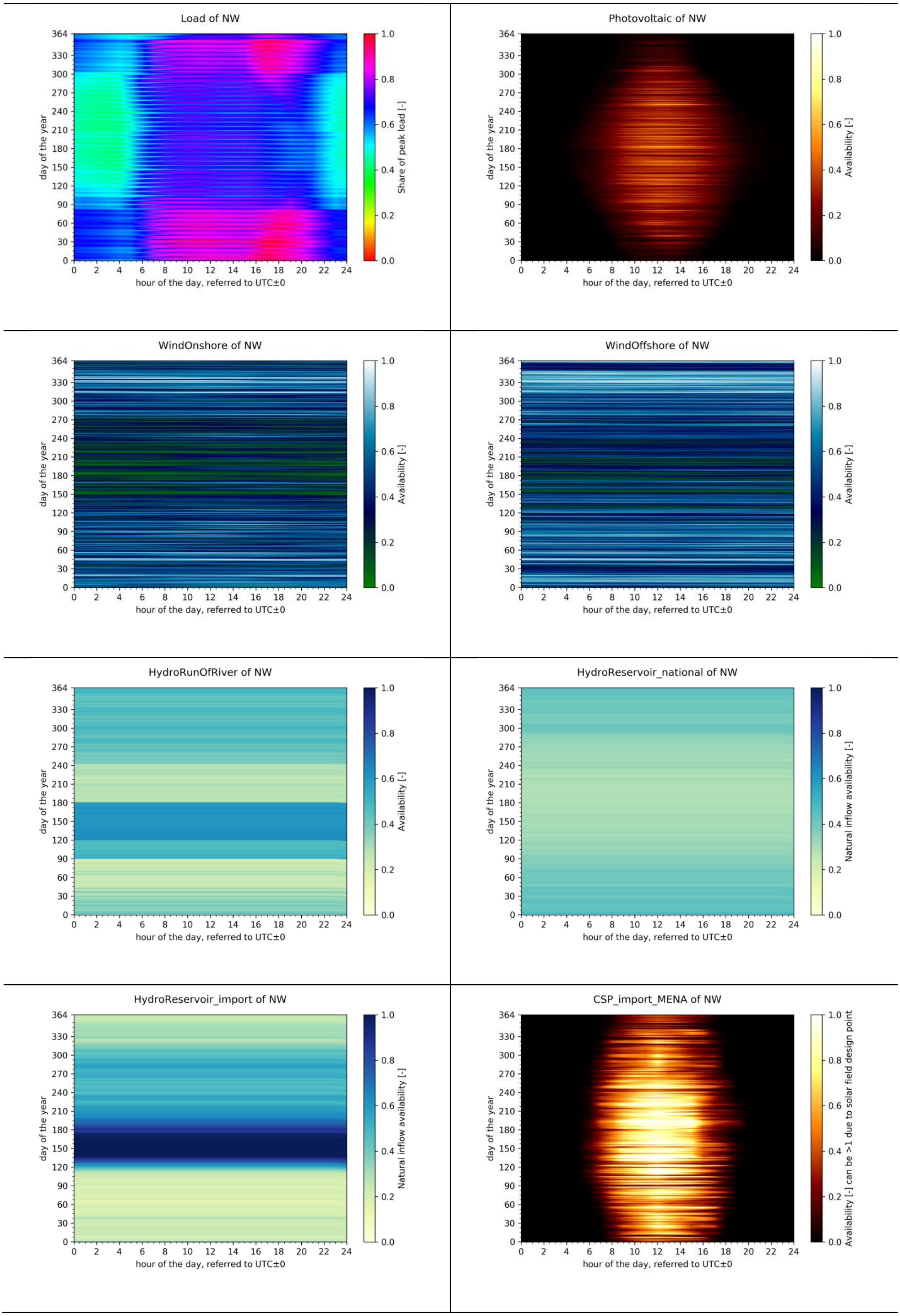

Figure 25: Load and technological time series of model region NW

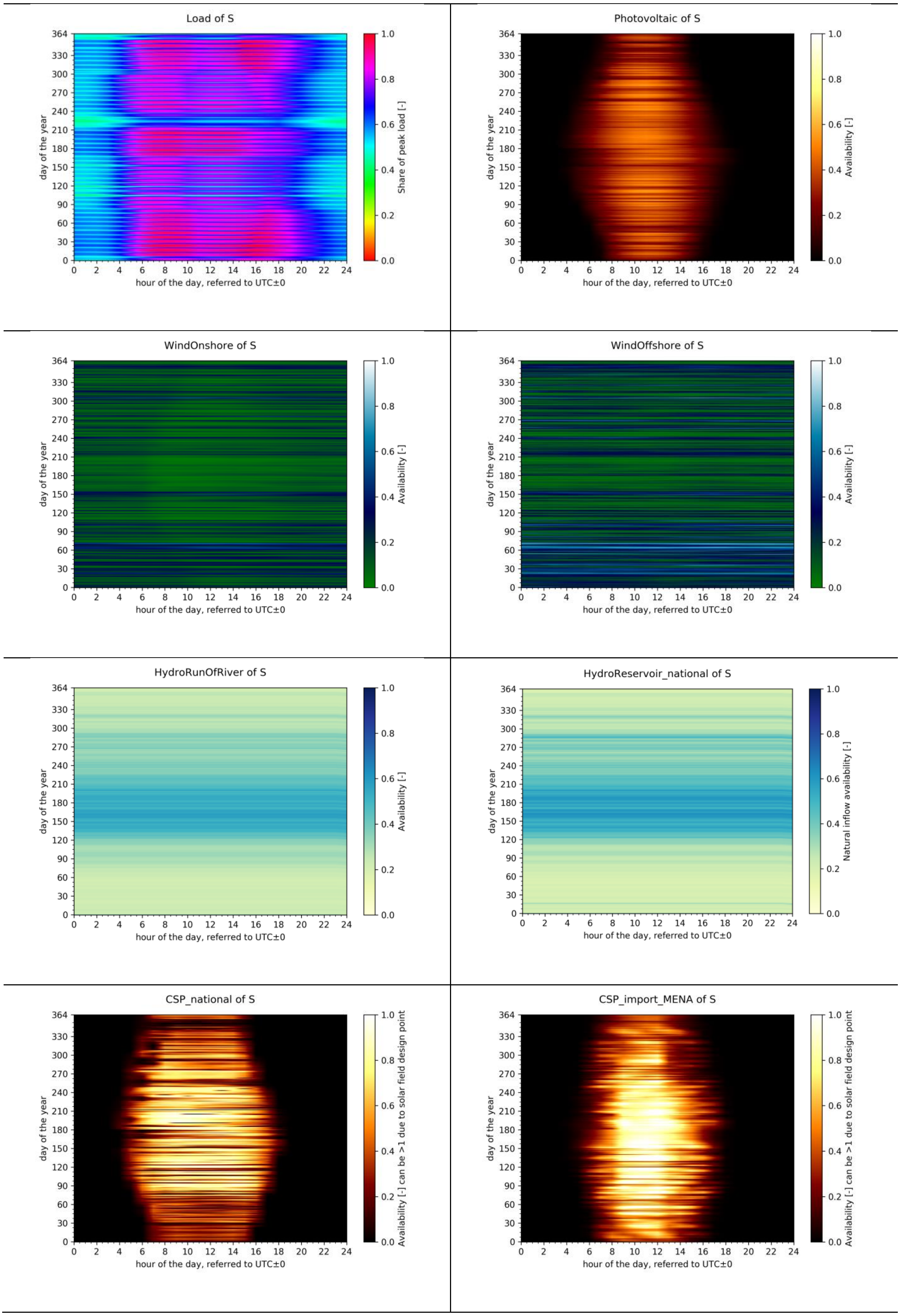

Figure 26: Load and technological time series of model region S

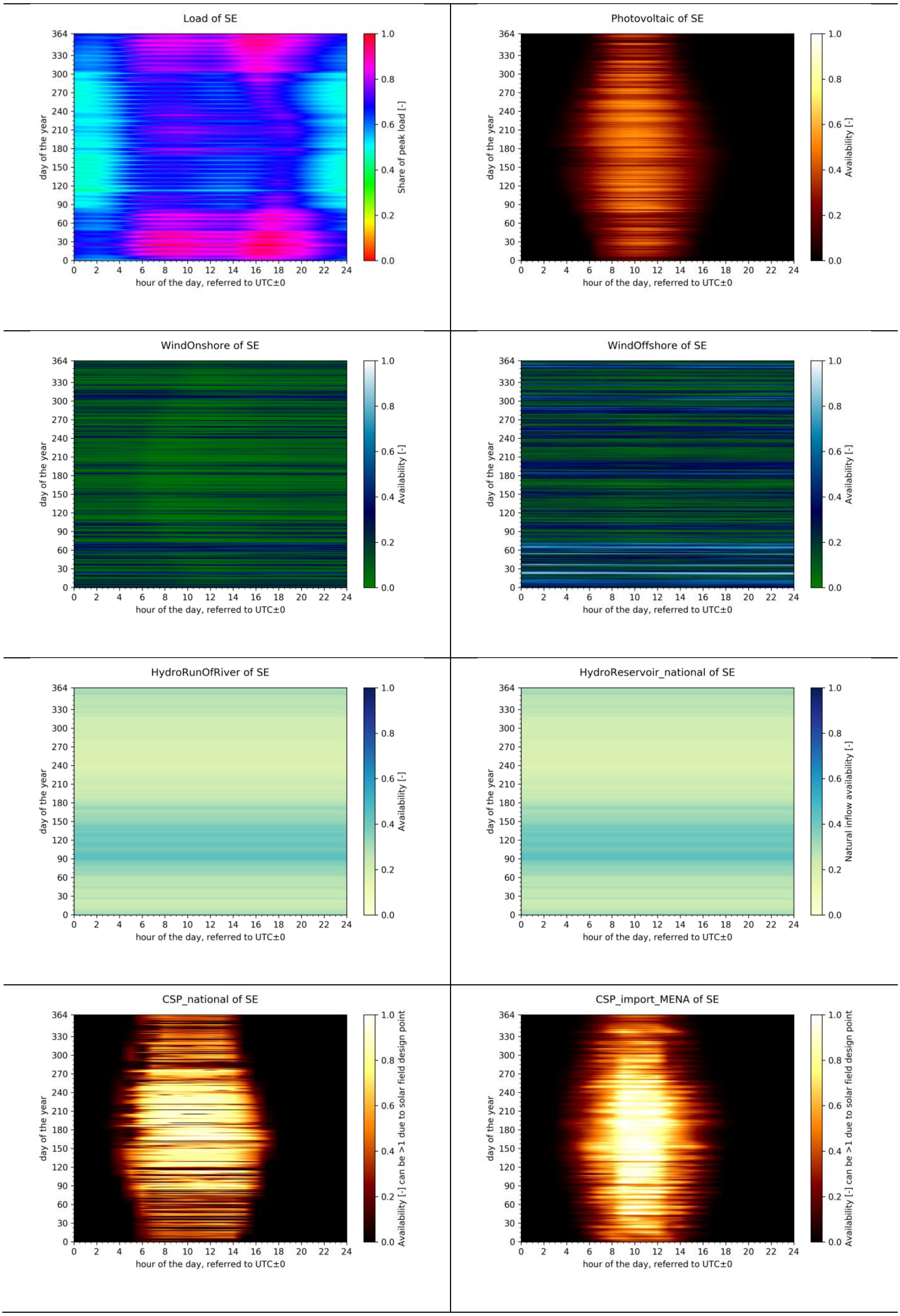

Figure 27: Load and technological time series of model region SE

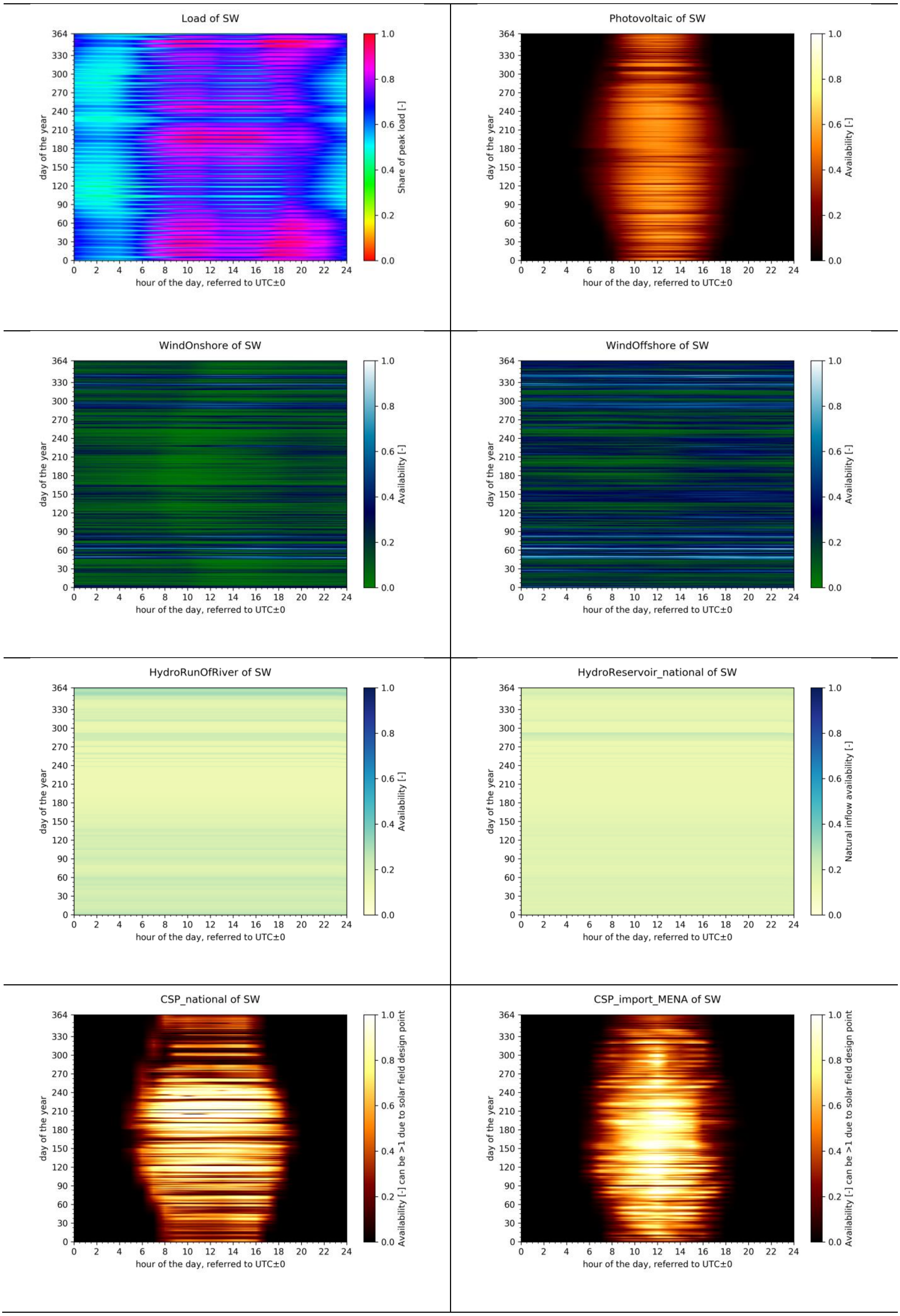

Figure 28: Load and technological time series of model region SW

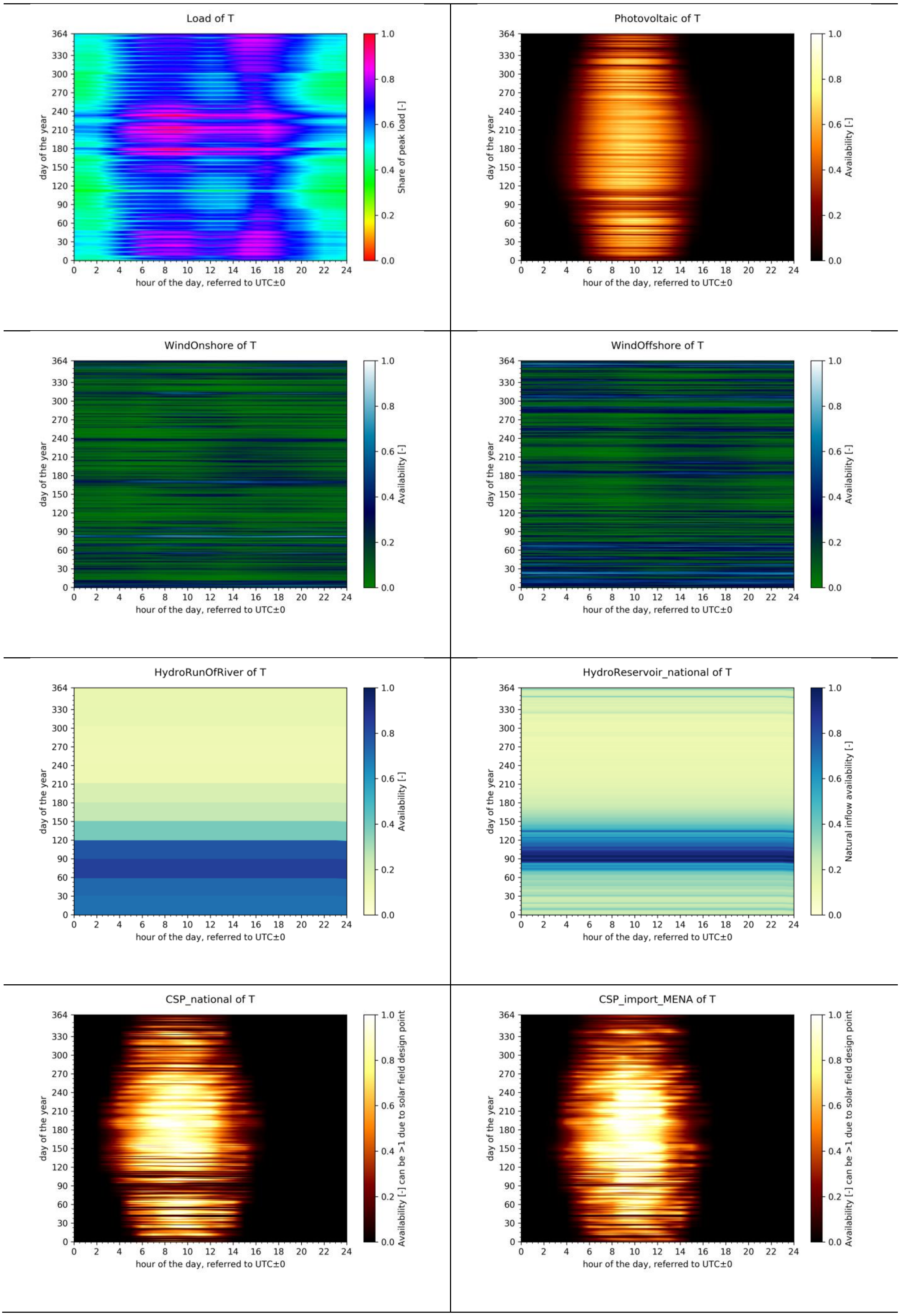

Figure 29: Load and technological time series of model region T

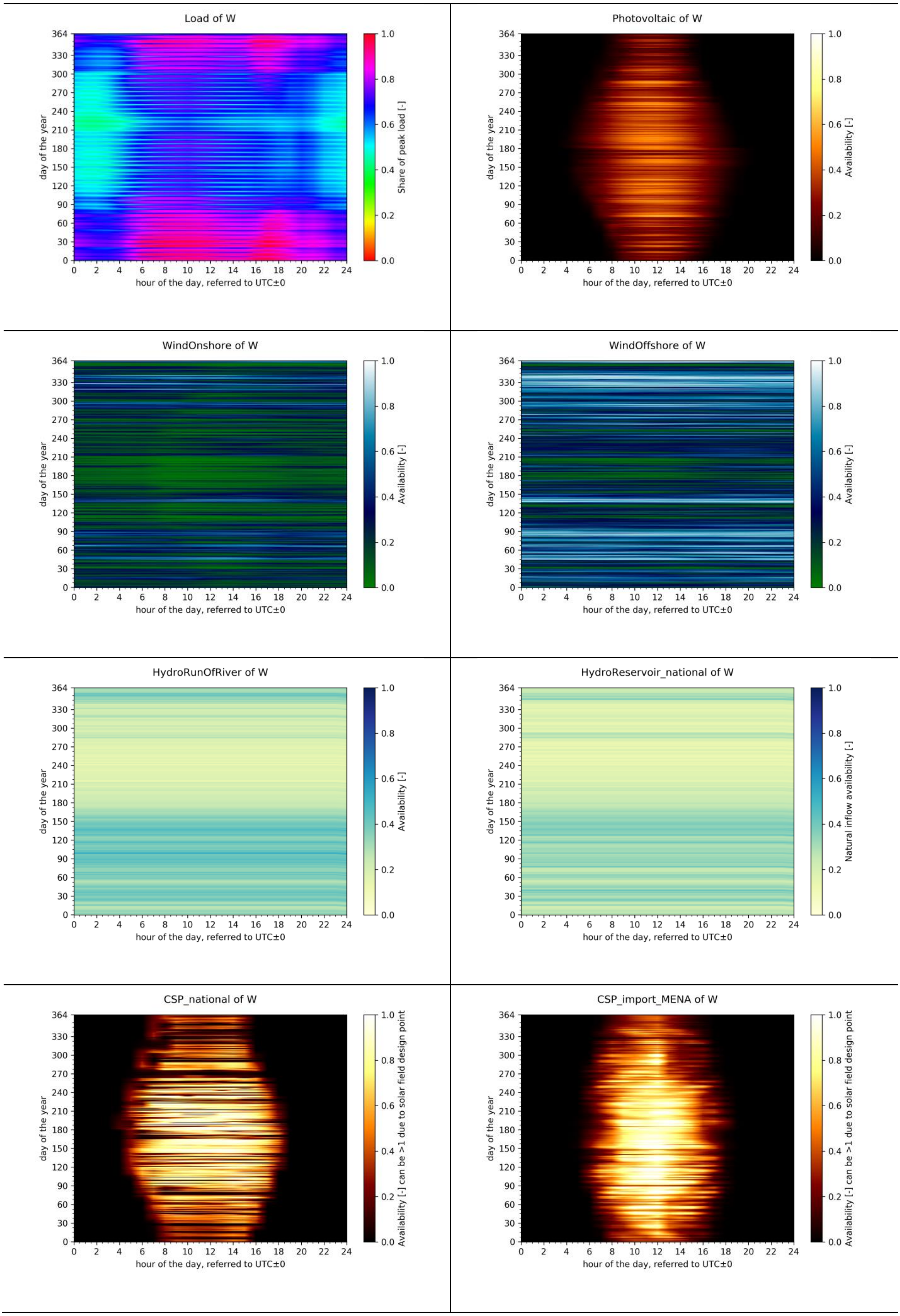

Figure 30: Load and technological time series of model region W

5.2.4 *Demand Side Management*

Regarding Demand Side Management (DSM), former studies have shown that the economic potential of DSM in Germany is approximately 10 GW [10] [37]. DSM substitutes short time storages (e.g. lithium ion batteries) and cost-efficient gas turbines [10] [37]. Thus, DSM has only a small influence on system cost and operating behaviour of the power plant park in Germany [10] [37]. Therefore DSM is neglected in the analysis.

5.2.5 *Storages*

The model uses different types of storage: short-term (e.g. battery type, represented by parameters for lithium ion batteries), medium-term (e.g. compressed air and pump storages) and long-term storages (e.g. hydrogen storages). The representatives are chosen due to the optimization method with the target function of minimizing system cost. When modelling technologies with about the same cost, the optimizer always uses the cheapest technology. Other technologies with about the same characteristics are therefore excluded by the optimizer. Thus, only the used three types of storage are considered due to their different temporal commitment.

Power-to-Gas-to-Power (P2G2P) is modelled with an electrolysis (alkali in maximum cost sensitivity, PEMFC in minimum cost sensitivity), methanation, compressed and stored in a salt cavern or in the gas distribution grid and burned in gas turbines. Power capacity of electrolyser and turbine can be optimized separately.

5.2.6 *Security of supply*

To ensure security of supply, the capacity credit is introduced (see Table 18). The capacity credit defines revision and outage of the installed capacity of each technology as an empirical value. For security and reserve reasons, the total firm capacity (product of capacity credits and related power plant capacities) must be 100%. So the total firm capacity is calculated referred to peak load at about 105%. To ensure firm national capacity in Germany, gas turbines are installed to cover the total peak demand together with other national dispatchable capacities in case of any failure. Installation of back-up capacities raise new financing questions if these capacities were not used (e.g. apportionment financing). CSP-HVDC is assumed with a capacity credit of 0% to model a possible total outage based on non-technical reasons. However, this dispatchable technology is able to ensure firm capacity due to its co-firing option. Thus, CSP-HVDC could substitute national gas turbines and reduce system cost if firm capacity abroad is accepted as such.

5.2.7 *Supply technologies and their resource potentials*

Table 12 shows the model limitations by resource potential of the listed technologies. Other used technologies or technological components (e.g. storage size) have unlimited potentials.

Table 12: Limited resource potentials of used technologies

Technology/ Model region	Pump storage discharge [MW_{el}]	Hydro run-of-river [MW_{el}]	Hydro-reservoir regional, turbine [MW_{el}]	Hydro-reservoir import from N, turbine [MW_{el}]*	Geothermal energy [TWh_{el}]	Solid biomass [TWh_{chem}]	CSP regional, solar field [GW_{th}]
G	15875	4377	430	6153	26	216	0
N	4781	39326	25813	-	1	832	0
E	3500	4504	963	3748	17	338	0
S	20014	31924	16500	-	18	317	105
W	7743	13943	11660	-	12	329	19
NW	3853	3507	328	7308	24	57	0
NE	2612	32448	0	-	1	2580	0
SE	4149	21721	8330	-	8	520	42
NAE	0	3033	0	-	13	12	242239
NAW	932	1724	0	-	9	80	234089
SW	19588	8560	12999	-	22	314	1566
T	571	14611	679	-	75	212	373
MES	0	3313	0	-	0	12	58426
I	0	1044	0	-	6	38	37867
ME	0	0	0	-	68	3	224692

*The import potential of hydro reservoir from model region N to G, E and NW is calculated with 40% of the available potential in N and distributed due to the electricity of the destination model regions. Thus, 60% of the original potential remains in model region N.

Potential of pump storage discharge is taken from [38] “T2 realisable (5km)” with energy to power ratio of 7 and a reduced potential of 75.5%. This reduced potential is achieved comparing the cost-efficient pump storage discharge potential in Germany of 15GW [39] to the study values with 20GW [38]. Potential of hydro run-of-river and CSP is taken from [2] for Europe and from [16] for MENA. Potential of hydro-reservoir is taken from [40] using a power plant matching in Europe and for Turkey from [2]. Potential of geothermal energy is taken from [21], [12] and for Germany from [41]. Net primary production (NPP) potential of solid biomass is taken from model values of [42]. The assumed usable energy potential consists of 25% of total tree NPP and of 20% of total straw NPP of the year 2010.

5.2.8 *Annual characteristic of load and renewable resources*

For a regional comparison of renewable resources and demand Table 13 shows peak load and average full load hours of model regions.

Table 13: Peak load and average resource full load hours of model regions

Model region	Peak Load [GW]	Average resource full load hours [h/y]					
		PV	Wind Onshore	Wind Offshore	Hydro Run Of River	CSP solar field national	CSP solar field import
G	112	836	2107	4125	5015	-	1934
N	99	867	2023	3810	4137	-	1980
E	69	1016	1731	3207	2396	-	2011
S	112	1139	1353	1917	3033	1914	1943
W	155	1027	2110	3626	2543	1881	1926
NW	134	789	3721	4309	3606	-	1916
NE	170	1011	2251	3260	3220	-	1939
SE	54	1118	1290	2265	2432	1938	1997
NAE	182	1747	1257	1939	4219	2135	-
NAW	112	1701	2179	3096	1925	2026	-
SW	57	1309	1555	2418	1551	2034	1897
T	113	1494	1312	1767	3266	1847	1966
MES	165	1620	1661	1400	4096	1881	-
I	152	1671	1591	1725	4957	1972	-
ME	170	1749	1577	1765	-	2105	-

The average resource full load hours are a result of an aggregation of the spatial availability of the resource. Full load hours of CSP solar field import represent an average of selected sites in EUMENA which leads to a more conservative approach than for CSP solar field national.

5.3 Exogenous assumptions for analysing the value of CSP-HVDC

In the second part for the scenario analysis exogenous capacities and parameters are used which are shown in Table 14 to Table 17.

Table 14: Exogenous capacities of CSP components

	CSP-HVDC				CSP			
Model region	**Power block [MW]**	**SM [-]**	**Solar field [$MW_{thermal}$]**	**Thermal energy storage [MWh]**	**Power block [MW]**	**SM [-]**	**Solar field [$MW_{thermal}$]**	**Thermal energy storage [MWh]**
G	40000	4.1	442213	1358331	0	0.0	0	0
N	6000	4.2	68506	191930	0	0.0	0	0
E	18000	3.5	171956	583796	0	0.0	0	0
S	28403	4.5	344970	980940	13409	2.9	104658	393059
W	60000	3.7	600805	2004039	1000	3.2	8737	28763
NW	60000	3.2	521139	1694940	0	0.0	0	0
NE	42562	3.9	453565	1429071	0	0.0	0	0
SE	9589	4.1	106843	311523	5834	2.7	41890	178021
NAE	0	0.0	0	0	162324	3.8	1668897	5449808
NAW	0	0.0	0	0	81748	4.0	875069	2602720
SW	3000	3.6	29007	97916	22264	3.0	179087	620259
T	50000	3.2	432586	1502329	7754	3.3	69768	238819
MES	0	0.0	0	0	150000	3.2	1287473	4728312
I	0	0.0	0	0	122061	3.8	1266472	4256975
ME	0	0.0	0	0	140242	3.4	1274001	4808231

Table 15: Exogenous capacities of power plants [MW_{el}]

Model region	**Photo-voltaic**	**Wind Onshore**	**Wind Offshore**	**Hydro Run Off River**	**Biomass**	**Geo-thermal**	**Gas turbine**
G	70000	70000	28000	4377	19000	4042	102500
N	50000	20000	8000	39326	33073	255	72400
E	50000	45000	30000	4504	17000	2500	57250
S	70000	60000	15000	31924	22500	2500	95000
W	120000	90000	25000	13943	32000	2112	138100
NW	70000	90000	10000	3507	5500	4711	138900
NE	120000	85000	18000	32448	60000	1800	91000
SE	35000	30000	15000	21721	12000	1069	44800
NAE	50000	15000	0	3033	1300	1800	48700
NAW	40000	20000	2000	1724	6000	1300	37200
SW	50000	30000	10000	8560	10000	3000	46950
T	50000	30000	0	14611	15000	13778	99700
MES	60000	0	0	3313	1300	0	44232
I	60000	0	0	1044	4000	1092	43900
ME	65000	0	0	0	300	10000	62800

Table 16: Exogenous capacities of hydro reservoir and pump storage plants [MW_{el}]

Model region	**Hydro reservoir turbine**	**Hydro reservoir pump**	***Hydro reservoir storage [MWh]***	**Import Hydro reservoir turbine**	**Import Hydro reservoir pump**	***Import Hydro reservoir storage [MWh]***	**Pump storage**	***Pump storage - storage [MWh]***
G	430	5284	*430000*	6153	18672	*6153000*	15875	*127000*
N	25813	25813	*25813000*	0	0	*0*	4781	*38248*
E	963	9953	*963000*	3748	10075	*3748000*	3500	*28000*
S	16500	23470	*16500000*	0	0	*0*	20014	*160112*
W	11660	46909	*11660000*	0	0	*0*	7743	*61944*
NW	328	5933	*328000*	7308	37220	*7308000*	3853	*30824*
NE	0	0	*0*	0	0	*0*	2612	*20896*
SE	8330	13814	*8330000*	0	0	*0*	4149	*33192*
NAE	0	0	*0*	0	0	*0*	0	*0*
NAW	0	0	*0*	0	0	*0*	932	*7456*
SW	12999	18980	*12999000*	0	0	*0*	19588	*156704*
T	679	13994	*679000*	0	0	*0*	571	*4568*
MES	0	0	*0*	0	0	*0*	0	*0*
I	0	0	*0*	0	0	*0*	0	*0*
ME	0	0	*0*	0	0	*0*	0	*0*

Table 17: Exogenous link capacities

Link according model regions	HVDC link capacity [GW]	380kV link capacity [GW]
G_N	2820	0
G_E	0	5367
G_S	0	7990
G_W	0	11045
G_NW	3450	0
N_NE	0	3196
N_E	3330	0
N_NW	3615	0
NE_E	0	3538
NE_SE	0	3347
NE_T	0	5206
NE_I	0	6402
NW_W	3555	0
NW_SW	3285	0
W_S	0	8603
W_NAW	10980	0
W_SW	0	2593
SW_NAW	0	10693
S_E	0	3065
S_SE	0	3226
S_NAE	9405	0
S_NAW	11115	0
SE_T	0	5156
SE_MES	7965	0
SE_NAE	9465	0
NAE_NAW	0	17356
NAE_T	11325	0
NAE_MES	0	14140
NAE_ME	10305	0
MES_I	0	11025
MES_ME	8805	0
MES_T	0	9829
I_T	0	8201
I_ME	7185	0
E_SE	0	3477

5.4 Used techno-economic data

The objective of the analysis is to model CSP-HVDC and CSP relative conservatively compared to other technologies. This facilitates a conservative examination of CSP-HVDC and CSP to analyse their value strictly avoiding an overestimation of this technology. Therefore the applied techno-economic data for other technologies are rather optimistic.

The bandwidth of cost assumptions ($€_{2015}$) and technological characteristics in Table 18 to Table 24 are assumed from today's point of view and can differ from reality especially when projecting an energy system in the year 2050.

Table 18 to Table 24 include an exchange rate with 1$ at the parity of 1.35 €. Some values are based on a time value of money the year 2010. Therefore an inflation rate of 10% is considered from 2010 to 2015 to calculate the time value of money of the year 2015. The mean values are not listed in the tables but are calculated according to the average of max and min values.

Table 18: Cost and technology parameters for power plants in the year 2050 based on expert assumptions

Technology	Cost sensi-tivity	Specific investment [k€/MWel]	O&M Fix [%/y] of investment	O&M Variable [€/MWh]	Fuel cost [€/MWh]	Amortisation Time [y]	Interest Rate	Efficiency [-] net	Availability	Capacity Credit [-]
Photovoltaics	max	1150	0.04	0.00		20	9%	1	98%	0
	min	597	1.10	0.00		40	3%			
Wind Onshore	max	1272	2.10	4.33		18	9%	1	95%	0
	min	769	1.61	2.44		24	3%			
Wind Offshore	max	2275	3.64	13.87		16	9%	1	95%	0
	min	1052	3.49	9.55		22	3%			
Run-Of-River	max	5541	5.50	4.84		40	9%	1	95%	0
	min	5541	2.75	2.44		60	3%			
Hydro Reservoir*	max	2113	5.00	1.00		40	9%	1	98%	0
	min	1017	5.00	1.00		30	3%			
Solid Biomass	max	3833	1.98	3.20	40.0	20	9%	0.35	90%	0.9
	min	1647	5.60	2.90	25.0	30	3%			
Geothermal	max	6797	3.00	0.10		20	9%	1	90%	0.9
	min	3826	3.00	0.10		30	3%			
CSP power block	max	1098	2.50	2.22		35	9%	0.37	95%	modelled with 0, however 0.9 is possible accepting firm capacity abroad
	min	857	2.50	2.22		45	3%			
CSP solar field	max	356 k€/MW$_{thermal}$	2.50			20	9%		95%	-
	min	166 k€/MW$_{thermal}$	2.50			30	3%			
CSP thermal storage	max	18 k€/MWh	2.50			20	9%	0.95 and 0.05%/h self-discharge rate	95%	-
	min	11 k€/MWh	2.50			30	3%			

Sources: [43], [44], [45], [46], [47], [48], [49], [50], [51], own assumptions

Table 19: Cost and technology parameters for storages in the year 2050

Technology	Cost sensitivity	Specific investment [k€/MWel]	O&M Fix [%/y] of investment	O&M Variable [€/MWh]	Amortisation Time [y]	Interest Rate	Efficiency [-] net	Availability	Capacity Credit [-]
Pump Storage storage	max	40 k€/MWh	2.80	-	30	9%	0%/h self-discharge rate		-
	min	5 k€/MWh	1.86	-	40	3%			
Pump Storage charge	max	400	2.80	3.80	20	9%	0.89	95%	-
	min	180	1.86	3.80	30	3%			
Pump Storage discharge	max	400	2.80	-	20	9%	0.90		0
	min	170	1.86	-	30	3%			
Power-to-Gas-to-Power (P2G2P) Storage	max	0.20 k€/MWh	3.00	-	25	9%	0%/h self-discharge rate		-
	min	0.20 k€/MWh	2.42	-	35	3%			
Power-to-Gas-to-Power (P2G2P) charge	max	1206 = 606 (alkali electrolysis) +600 (methanation)	3.00	2.30	15	9%	0.70 = 0.79 (methanation) x 0.89 (compression)	95%	-
	min	922 = 322 (PEM electrolysis) +600 (methanation)	2.42	1.64	20	3%			
Power-to-Gas-to-Power (P2G2P) discharge (gas turbine)	max	713	3.00	-	25	9%	0.465		0.95
	min	417	2.42	-	40	3%			
Compressed Air Storage storage	max	60 k€/MWh	1.30	-	25	9%	0.125%/h self-discharge rate		-
	min	38 k€/MWh	1.30	-	35	3%			
Compressed Air Storage charge	max	310	1.30	2.70	20	9%	0.88	95%	-
	min	200	1.30	0.10	30	3%			
Compressed Air Storage discharge	max	400	1.30	-	25	9%	0.70		0
	min	260	1.30	-	35	3%			
Lithium Ion storage	max	220 k€/MWh	2.00	-	15	9%	0.001%/h self-discharge rate		-
	min	150 k€/MWh	2.00	-	25	3%			
Lithium Ion charge	max	25	2.00	0.22	15	9%	0.97	95%	-
	min	12.5	2.00	0.22	25	3%			
Lithium Ion discharge	max	25	2.00	-	15	9%	0.97		0
	min	12.5	2.00	-	25	3%			

Sources: [43], [52], [53], [54], own assumptions

Table 20: Cost and technology parameters for carbon emitting and nuclear technologies in the year 2050

Technology	Cost sensitivity	Specific investment [k€/MWel]	O&M Fix [%/y] of investment	O&M Variable [€/MWh]	Fuel cost [€/MWh$_{chem}$]	Amortisation Time [y]	Interest Rate	Efficiency [-] net	CO_2 sequestration [-]	Availability	Capacity Credit [-]
Coal CCS Steam Turbine	max	2460	4	9.2	30	25	9%	0.299	0.85	0.896	0.9
	min	1807	4	9.2	18.9	40	3%				
Coal Steam Turbine	max	1418	4	0.1	30	25	9%	0.509	0	0.896	0.9
	min	1108	4	0.1	18.9	40	3%				
Combined CCS Cycle Gas Turbine	max	1203	4	3.5	65.2	25	9%	0.428	0.86	0.96	0.9
	min	867	4	3.5	40.1	40	3%				
Combined Cycle Gas Turbine	max	691	4	0.3	65.2	25	9%	0.621	0	0.96	0.9
	min	491	4	0.3	40.1	40	3%				
Gas Turbine	max	713	4	0.3	65.2	25	9%	0.465	0	0.95	0.9
	min	417	4	0.3	40.1	40	3%				
Lignite Steam Turbine	max	1750	4	0.1	11.1	25	9%	0.491	0	0.902	0.9
	min	1250	4	0.1	9.1	40	3%				
Nuclear Steam Turbine	max	13030	4	0.1	5.5	25	9%	0.309	-	0.90	0.9
	min	4684	4	0.1	5	40	3%				

Sources: [51], [55], [56], [57], own assumptions, CCS O&M Variable are based on cost for CO_2 transport (3€/t) and CO2 storage (4.45 €/t) [58]

Table 21: Specific CO_2 emission

Fuel	tCO_2/MWh_{chem}
Coal	0.3348
Lignite	0.3996
Natural Gas	0.2016
Nuclear	0
Biomass	0

Source: [51]

Table 22: CO_2 certificate cost representing environmental impact

Cost sensitivity	€/tCO_2
max	82.5
mean	62.7
min	49.5

Source: [51]

Table 23: Techno-economic parameters of HVDC infrastructure

	DC	**DC converter**	**Losses**
OHL	786.000 €/km	148.730.000 € per station	4.5 %/1000km
UGC	2.271.350 €/km	148.730.000 € per station	3.5 %/1000km
Sea cable	2.672.000 €/km	148.730.000 € per station	2.7 %/1000km
Specific Capacity	1500 MW	1500 MW	
Specific Voltage	600 kV		

Losses of converter station are assumed with 0.7%. Sources: [59], [25], [13].

Table 24: Learning curve approach of CSP solar field, thermal storage and power block based on installed capacity and progress ratio

Cost sensitivity	Unit	Current state	MAX	MEAN	MIN	Unit	Progress Ratio MAX	Progress Ratio MIN
year		2015	2050	2050	2050			
Installed capacity	MW	4,700	120,000	835,000	1,550,000			
Solar Field	[k€/MW_{th}]	647	355	260	166	[-]	0.88	0.85
Thermal Storage	[k€/MWh_{th}]	50	19	15	11	[-]	0.80	0.83
Power Block	[k€/MW_{el}]	1206	1098	978	857	[-]	0.98	0.96

Sources: based on [60] and [25], [61], [62], [63]

Table 25: Used parameters for distribution and transmission grid inside a model region

Grid	**Distribution grid**						**Transmission grid**				
	Start of grid expansion [% of peak load]			**cost per fluc feed-in [€/kW]**			**Start of grid expansion [% of peak load]**			**cost per fluc feed-in [€/kW] (OHL)**	**cost per fluc feed-in [€/kW] (UGC)**
Cost scenario	max	mean	min	max	mean	min	max	mean	min	max/ mean/min	max/ mean/min
G	53.5	60.5	73.4	409	375	500	20	25	30	584	899
N	53.5	60.5	73.4	409	375	500	20	25	30	801	1233
E	53.5	60.5	73.4	409	375	500	20	25	30	824	1269
S	53.5	60.5	73.4	409	375	500	20	25	30	647	997
W	53.5	60.5	73.4	409	375	500	20	25	30	582	896
NW	53.5	60.5	73.4	409	375	500	20	25	30	481	741
NE	53.5	60.5	73.4	409	375	500	20	25	30	1149	1769
SE	53.5	60.5	73.4	409	375	500	20	25	30	1253	1929
NAE	53.5	60.5	73.4	409	375	500	20	25	30	1331	2049
NAW	53.5	60.5	73.4	409	375	500	20	25	30	1939	2985
SW	53.5	60.5	73.4	409	375	500	20	25	30	1294	1991
T	53.5	60.5	73.4	409	375	500	20	25	30	1159	1783
MES	53.5	60.5	73.4	409	375	500	20	25	30	1288	1982
I	53.5	60.5	73.4	409	375	500	20	25	30	1227	1889
ME	53.5	60.5	73.4	409	375	500	20	25	30	517	795

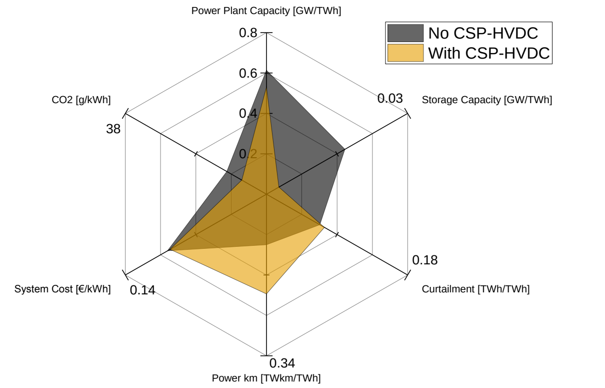

E - Small CO_2 EUMENA exoGrid

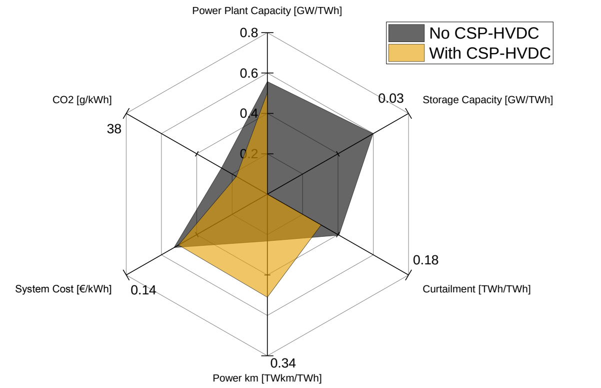

G - Small CO_2 EUMENA exoGrid

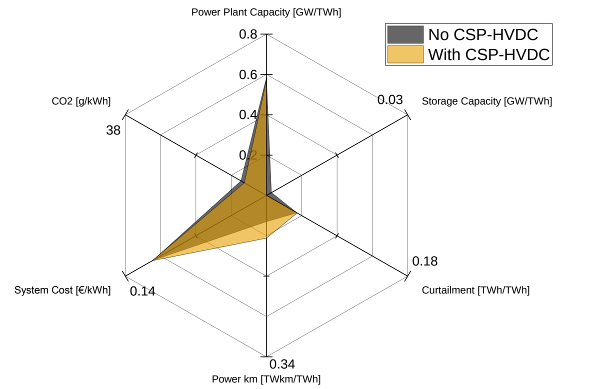

N - Small CO_2 EUMENA exoGrid

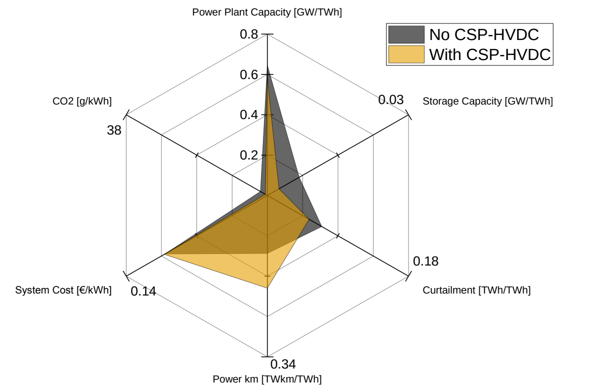

NE - Small CO_2 EUMENA exoGrid

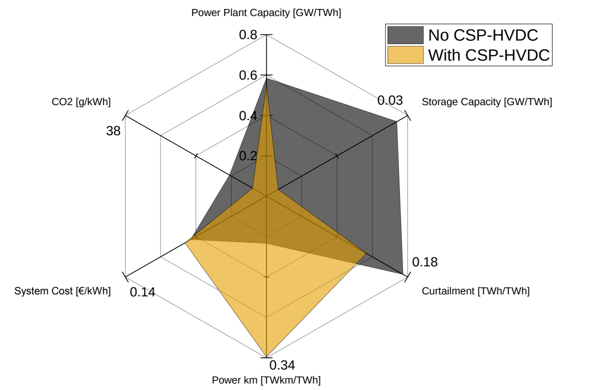

NW - Small CO_2 EUMENA exoGrid

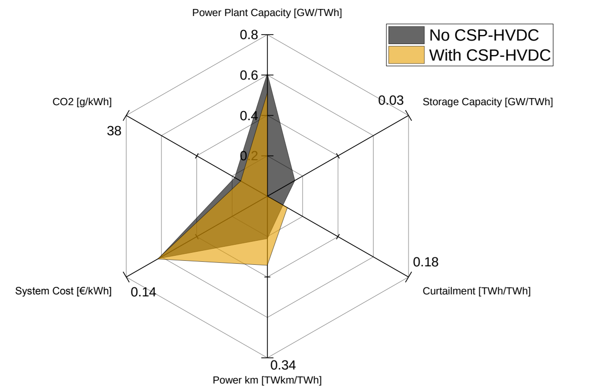

S - Small CO_2 EUMENA exoGrid

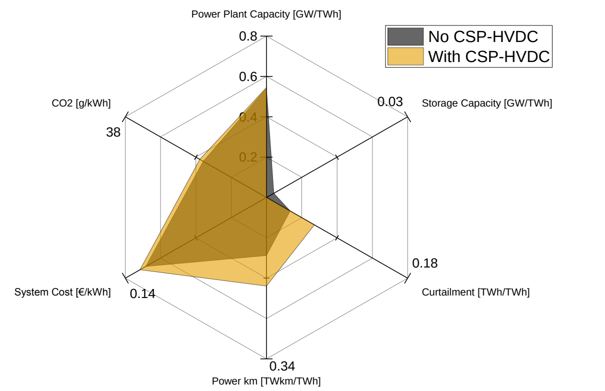

SE - Small CO_2 EUMENA exoGrid

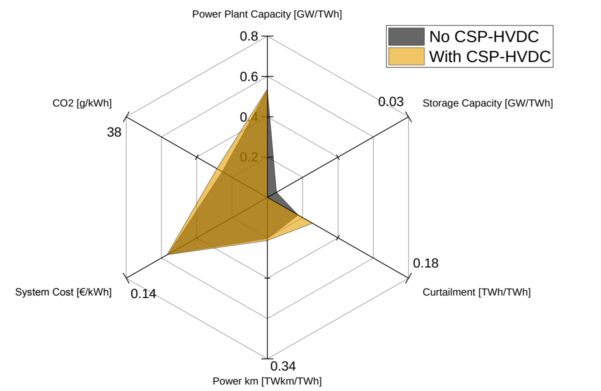

SW - Small CO_2 EUMENA exoGrid

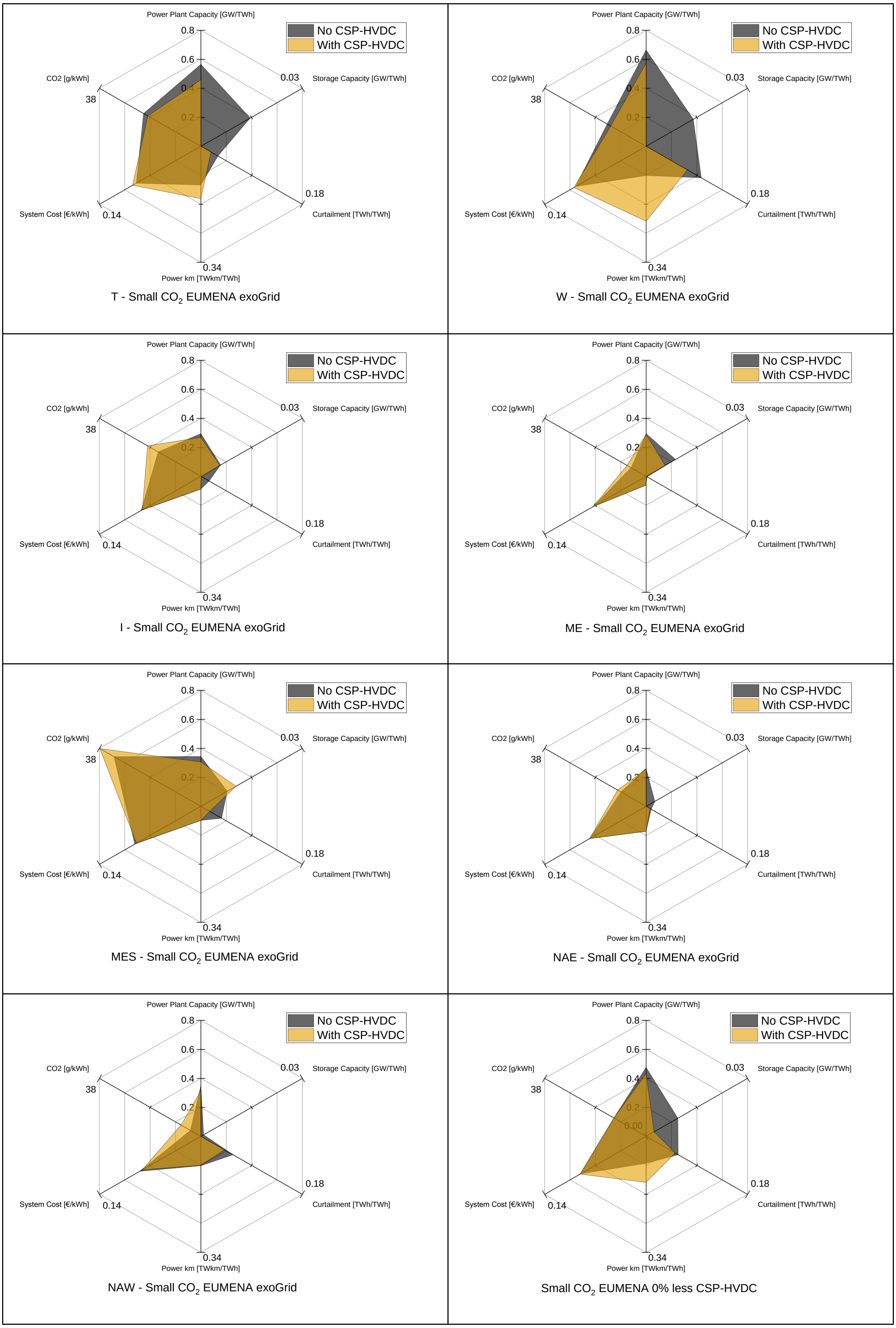

Figure 31: Scenario with maximum set CSP-HVDC capacity (CSP-HVDC base scenario)